Water Entry Study of the MK 25 Torpedo with 3.5-Caliber 70-Degree Spherogive Head

A Joint Study

G. M. Wilcox
Hydrodynamics Laboratory
California Institute Technology

J. G. Waugh
U. S. Naval Ordnance Test Station
Pasadena Annex

DEPARTMENT OF THE NAVY
Bureau of Ordnance Contract NOrd 9612
Buord Task Assignment NOTS-21-Re6a-220-8
Office of Naval Research Local Project 329

Hydrodynamics Laboratory
Report No. E-12.12
Copy No. 48

WATER ENTRY STUDY OF THE MK 25 TORPEDO WITH 3.5-CALIBRE 70-DEGREE SPHEROGIVE HEAD

A Joint Study

G. M. Wilcox
Hydrodynamics Laboratory
California Institute of Technology

J. G. Waugh
U. S. Naval Ordnance Test Station
Pasadena Annex

Department of the Navy
Bureau of Ordnance Contract NOrd 9612
BuOrd Task Assignment NOTS-21-Re6a-220-8
Office of Naval Research Local Project 329

Report No. E-12.12
May 1953
Pasadena, California

CONTENTS

FOREWORD

The cooperative study reported herein is the first phase of an extensive investigation of the modeling of water entry phenomena that was planned and executed jointly by the Hydrodynamics Laboratory of the California Institute of Technology and the Naval Ordnance Test Station. In this study, for the first time, full-scale launchings were planned specifically for correlation with model experiments.

The test facilities for water entry studies of both the Naval Ordnance Test Station and the Hydrodynamics Laboratory were necessary for this investigation. These facilities, all located in the Pasadena area, complement each other and, together, make up a complete and very unique set of test apparatus. In addition to the full-scale ranges at Morris Dam, the Naval Ordnance Test Station now has a small Variable Angle Variable Pressure model tank. This tank is equipped for precision measurement of whip and for detailed photographic observation of the cavity and the missile during the first two lengths of underwater travel. The larger model tank of the Hydrodynamics Laboratory is instrumented for precise determination of the trajectory, orientation of the missile, and general cavity behavior over twenty or more lengths of underwater travel.

This study was conducted under the general supervision of Dr. Raymond W. Ager of Naval Ordnance Test Station and of the undersigned. Dr. John G. Waugh of Naval Ordnance Test Station and Miss Genevieve M. Wilcox of the California Institute of Technology were in direct charge of the work and maintained close liaison throughout the study. Most of the work of writing and organizing this report was done by Miss Wilcox.

Joseph Levy
Section Chief
Hydrodynamics Laboratory

ABSTRACT

This report describes a study conducted jointly by the Hydrodynamics Laboratory of the California Institute of Technology and the Pasadena Annex of the Naval Ordnance Test Station, Inyokern. Air to water launchings were made with a full-size (22.42-in. dia.) dummy Mk 25 aircraft torpedo with a 3-1/2-cal. 70° spherogive nose and with a 2-in. dia. model of the same shape.

The purpose of this investigation was to study the problems associated with water entry modeling. Froude scaling was used to determine model entry velocity and the air pressure in the model system was reduced until the cavitation number of the model equaled that of the prototype.

Equal cavitation number and equal Froude number scaling was found to be adequate as long as a turbulent boundary layer existed in the flow around the model. When the entry velocity of the model was low enough for a laminar boundary layer to occur, the trajectory of the model deviated from that of the prototype beyond 35 diameters of underwater travel. It was then necessary to induce turbulence in the boundary layer by roughening the nose of the model before successful modeling could be achieved.

The tests made during this investigation were with the following entry conditions:

Entry Velocity	prototype	- 200 fps and 400 fps
	model	- 60, 80 and 120 fps
Air Pressure	prototype	- 1 atm.
	model	- 1, 1/11 and 1/21 atm.
Air Trajectory	prototype and model	- 22°
Entry Pitch Angle	prototype	- 0 to 6° nose up
	model	- 3° nose down to 6° nose up

INTRODUCTION

This report describes a series of aircraft torpedo launchings made by the Pasadena Annex of the Naval Ordnance Test Station, Inyokern, and the Hydrodynamics Laboratory of the California Institute of Technology. The projectile used in these tests was a dummy Mk 25 aircraft torpedo with a 3-1/2-cal. 70° spherogive head. The Naval Ordnance Test Station launched both a full-size (22.42-in. dia.) torpedo and a 2-in. dia. model of the same shape. The tests at the Hydrodynamics Laboratory were with the 2-in. dia. model only. The launchings made at the Naval Ordnance Test Station were under the sponsorship of Bureau of Ordnance Task Assignment NOTS-21-Re6a-220-8 and Office of Naval Research Local Project 329, and those at the Hydrodynamics Laboratory under Bureau of Ordnance Contract NOrd 9612.

The purpose of these tests was to investigate the problem of the water entry behavior of a fine nose aircraft torpedo under a wider range of conditions than used heretofore. This study is part of a larger program planned for joint investigation by the Hydrodynamics Laboratory and the Naval Ordnance Test Station.

THE PROJECTILE

A fine nose projectile was used during these tests because the behavior of such a shape is extremely sensitive to variation of entry conditions.[1, 2*] The 3-1/2-cal. 70° spherogive nose was chosen primarily because a prototype was available. Water tunnel tests have shown that the separation of the cavity from the 3-1/2-cal. 70° spherogive nose might occur either on the spherical portion or on the ogive,[3] which would tend to make this shape sensitive to small variation in the conditions which determine the cavity. Figure 1 shows photographs of the model and of the prototype, as well as a line drawing showing the dimensions of the shape in terms of diameters. The model was scaled in accordance with the Froude law to be dynamically and geometrically similar to the prototype. The surface of the prototype was machined to an average roughness of approximately 40 to 60 microinches and painted with zinc chromate (ZnCr04). The model was polished to an average surface roughness of about 12 microinches. For the tests at the Hydrodynamics Laboratory, the model was covered with a coat of white baked enamel 0.001 in. thick. The painted surface of the model was held to the specified contour tolerance of ± 0.001 in. The paint

*See bibliography at end of report.

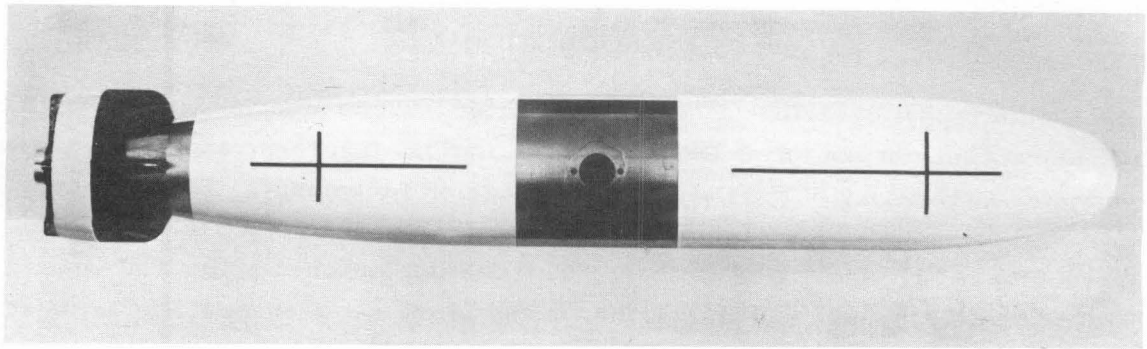

(a) 2-in. dia. model.

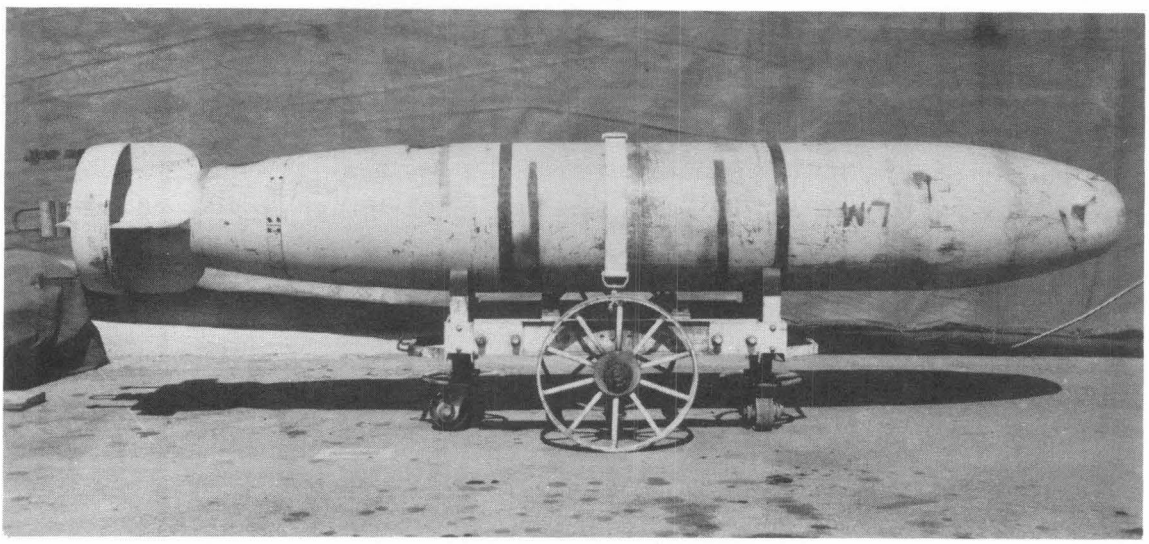

(b) 22.42-in. dia. prototype.

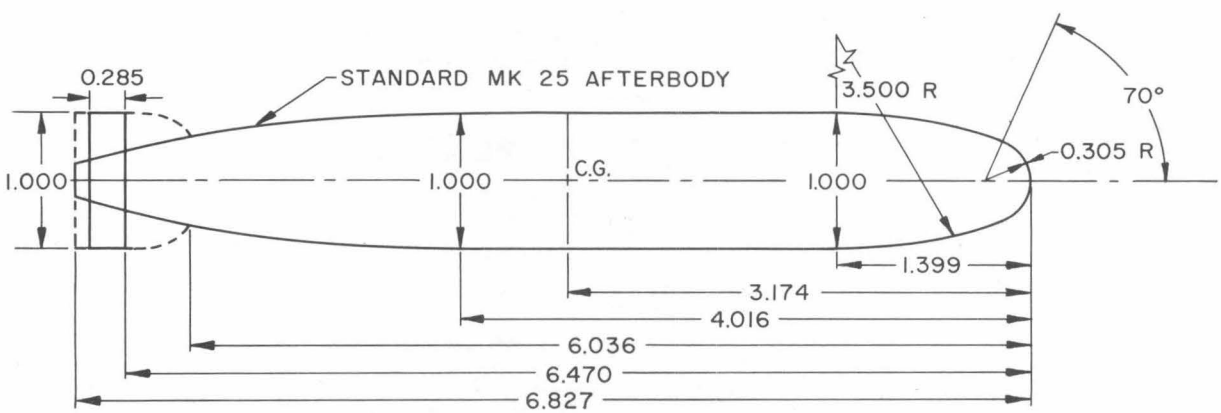

(c) Dimensions of torpedo given in diameters.

Fig. 1 - The Mk 25 aircraft torpedo with 3-1/2-cal. 70^{o} spherogive nose.

was removed from the model before the tests at the Naval Ordnance Test Station. Hence, the contour of the model was 0.001 in. under size for these tests. Table I lists the physical properties of the torpedoes and the tolerances maintained in their machining and correlation.

TABLE I - MODEL AND PROTOTYPE DIMENSIONS

	Prototype*	Model	
		Required by Froude Scaling	Model Used
Diameter - inches	22.42 + 0.020 - 0.010	2.000	2.001 ± 0.0002
Length - inches	152-1/8 ± 1/8	13.654	13.645 ± 0.005
Weight - pounds	between 1640 and 1675 ± 1/2	1.186	1.190 ± 0.005
Distance from c.g. to nose tip	between 71 and 73-1/8 ± 1/4	6.522	6.514 ± 0.02
Moment of inertia about transverse axis through c.g.	between 770.9 and 798.1 ± 5 slug ft^2	0.1436	0.1436 ± 0.001 lb/ft^2
Contour Tolerance - inches on radius	± 0.040		± 0.001

* The internal instrumentation was not the same for all of the prototype launchings, hence the weight, c.g. location and moment of inertia varied slightly.

TEST FACILITIES

The prototype was launched from the Variable Angle Launcher at the Morris Dam Launching Range. The model was launched in the small Variable Pressure Variable Angle Tank at the Naval Ordnance Test Station, Foothill, and in the large Controlled Atmosphere Launching Tank at the Hydrodynamics Laboratory. These facilities are fully described in references 4 through 7 listed in the bibliography.

TEST CONDITIONS

The entry conditions of the individual tests used in this report are tabulated in the appendix. The prototype was launched with nominal entry velocities of 200 and 400 fps, and the model at nominal velocities of 60, 80 and 120 fps. The model velocities of 60 and 120 fps were Froude-scaled from those of the prototype. All of the tests were made with a nominal air trajectory of 22°. The pitch of the prototype at water entry varied between 0° and 6° nose-up with respect to the trajectory, and the pitch of the model varied between 3° nose-down and 6° nose-up. All of the prototype tests were made at full atmospheric pressure; the model tests were made at air pressures of 1, 1/11 and 1/21 atm. For several of the launchings the nose of the model was artificially roughened with grains of sand 0.030 ± 0.002 in. in dia. Five of the launchings were made in the Naval Ordnance Test Station tank after aerosol had been added to the water. This reduced the surface tension of the water from 76 to 40 dynes/cm.

DISCUSSION OF RESULTS

Modeling Technique

Froude* scaling has long been accepted as a basis for modeling various phenomena associated with the motion of the free surface of a liquid because the forces of gravity and inertia are paramount in determining the free surface. Water entry, however, is very complex and Froude scaling alone is not adequate.

If the model and prototype tests are both conducted at full atmospheric pressure, the cavitation numbers** of the two systems will differ. Since the growth of a cavity is largely influenced by the cavitation number, it is reasonable to assume that the air pressure in the model system must be reduced until the cavitation numbers become equal before similar cavities can exist.[1] Test data taken during both this and previous investigations show equal cavitation number-Froude modeling to be considerably more valid than Froude modeling at any other cavitation number thus far studied. Hence, the restriction of equal cavitation numbers has been imposed in addition to Froude scaling in the modeling of water entry.

Heretofore it has been assumed that the nature of the boundary layer flow had no affect upon the flow in water entry because only a small portion of the missile surface is wetted. This investigation has shown that the boundary layer

---

* $F = v^2/\ell g \sim \frac{\text{inertia forces}}{\text{gravity}}$

** $K = \Delta p / \frac{1}{2} \rho v^2$

of the flow around the model must be considered. Equal cavitation number-Froude scaling did not cause valid modeling unless the boundary layer was turbulent. Roughness cannot be scaled as an ordinary linear dimension in a Froude system because the thickness of the boundary layer is a function of Reynolds number.* On the prototype both the Reynolds number and the roughness are sufficiently great to insure a turbulent boundary layer; the model surface is smooth and the Reynolds number relatively low, making a laminar boundary layer possible. The transition from laminar to turbulent boundary layer occurs on the model with the 3-1/2-cal. 70° spherogive nose at an entry velocity between 60 and 120 fps. With a blunter nose the critical velocity would be lower, as a turbulent boundary layer occurs more readily on a blunt shape.

A turbulent boundary layer was induced artificially on the 3-1/2-cal. 70° spherogive nose by roughening the nose with grains of sand 0.030 in. in dia. When the nose was roughened, the equal cavitation number-Froude scaling caused valid modeling. When the entry velocity of the model was increased until a turbulent boundary layer naturally existed, the presence of the roughness made no difference in the behavior of the model; the model with and without the roughness reproduced the behavior of the prototype.

Comparison of Model and Prototype Behavior

Since the entry angles of all of the prototype launchings and several of the model launchings were determined to only $\pm 1^{\circ}$, it is not possible to compare the results from individual tests. Instead, groups of tests are compared and the bands covered by groups of trajectories are shown rather than individual trajectories.

Tests with Entry Velocities of 200 fps for the Prototype and 60 fps for the Model

Figure 2 shows the trajectories of the smooth model at air pressures of 1, 1/11 and 1/21 atm. compared with the prototype trajectories from launchings having approximately the same entry pitch angles. The model trajectories at 1/11 atm. bear a greater resemblance to those of the prototype than do the trajectories obtained at the other two pressures. One-eleventh atmosphere is the pressure which causes the cavitation number in the model system to equal that of the prototype.

Although the results from the model tests at 1/11 atm. are in best agreement with the prototype, the model does not reproduce the behavior of the

---

*$R = vd\rho/\mu \sim \frac{\text{inertia forces}}{\text{viscous forces}}$

prototype beyond 35 dia. from water entry. The prototype trajectories are concave upward, while the model trajectories are concave downward. Figures 3 and 4 show groups of trajectories made with entry pitch angles ranging between 0° and 3° nose-up, and 4° and 6° nose-up, respectively.

Figure 5 compares the same prototype trajectories shown in Fig. 3 with model trajectories obtained at an air pressure of 1/11 atm. after the nose of the model has been artificially roughened. The various areas of roughness used in these tests are shown in Fig. 6. Roughness (a), where the sand was stuck on the nose tip, did not make much difference in the trajectory of the model. When the roughened area was increased slightly to that of roughness (b), the model trajectories became concave upward like those of the prototype. Within the accuracy of the prototype data, the rough-nose model reproduced the trajectory of the prototype. Roughness (c), where the sand was stuck on the ogive, did not produce valid modeling.

Figure 7 compares the trajectories of the roughened model with the prototype trajectories from Fig. 4. The model trajectories are still somewhat concave downward. The model with the roughened nose (Type b) deviated from the prototype beyond 40 dia. from water entry and the model with the entire ogive roughened (Type e) deviated from the prototype after 60 dia. of horizontal travel. The lack of agreement between the model and the prototype can be attributed to two factors.

The first factor is that it was necessary to induce a nose-up pitch velocity of about 50 deg/sec during the air flight of the prototype in order to obtain the flat entry pitch angles, while the model had a nose-down pitch velocity of 10 to 20 deg/sec (an absolute difference of approximately 70 deg/sec in the pitch velocities during air flight). Since this nose shape is very sensitive to change in other entry conditions, it is probably sensitive to difference in pitch velocity as well.

The second, and probably more important factor, is that it becomes difficult to induce a turbulent boundary layer by artificial means when the entry pitch angle is so flat that the ogival portion of the nose enters the water before the spherical tip is wetted. Under this condition roughness on the tip of the nose appears to be inadequate. Roughening the ogive did not produce satisfactory results either. The presence of the sand on the ogive increased the drag,* which caused the velocity to diminish more rapidly. Since the trajectory of this model becomes steeper as its entry velocity decreases,** it is reasonable

---

*See page 14.

**See page 29.

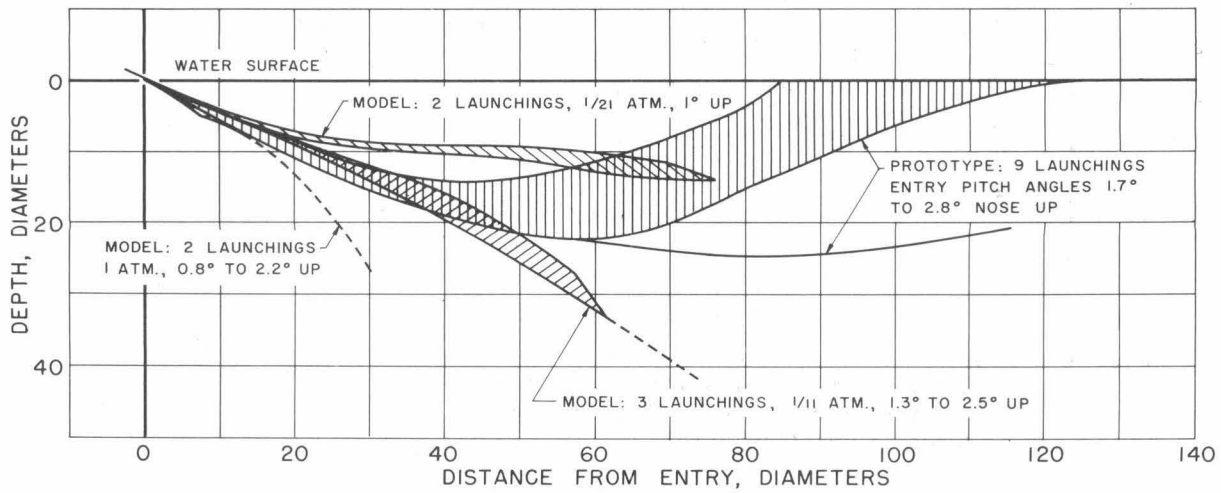

Fig. 2 - Underwater trajectories - Entry pitch angles 1^{o} to 3^{o} nose up.
Froude scaled model entry velocity: 60 fps.
Prototype entry velocity: 200 fps.
Various cavitation numbers in model system.

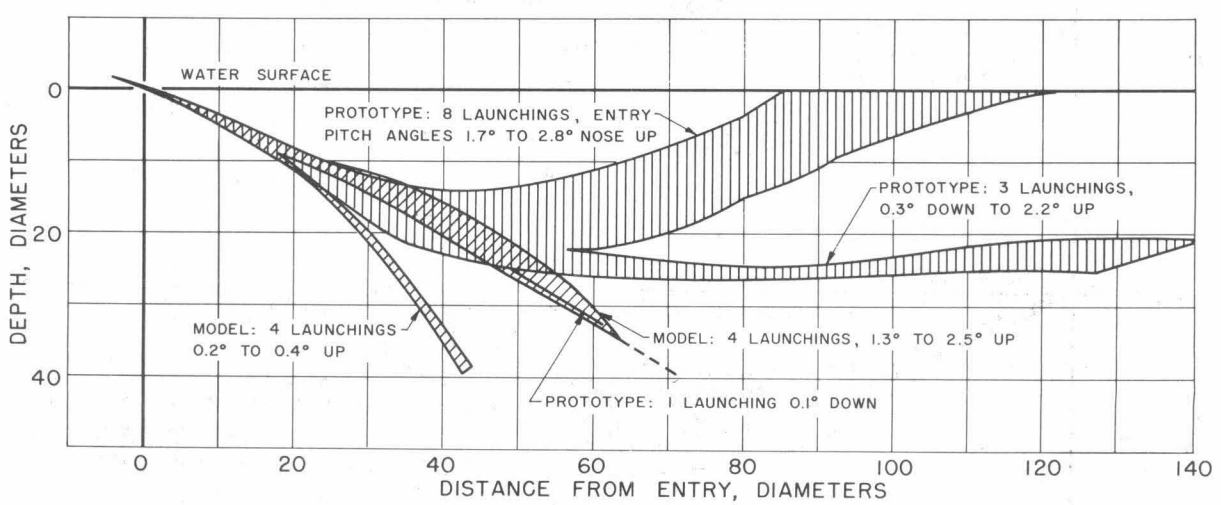

Fig. 3 - Underwater trajectories - Entry pitch angles 0^{o} to 3^{o} nose up.
Froude scaled model entry velocity: 60 fps.
Prototype entry velocity: 200 fps.
Equal cavitation numbers in model and prototype systems.

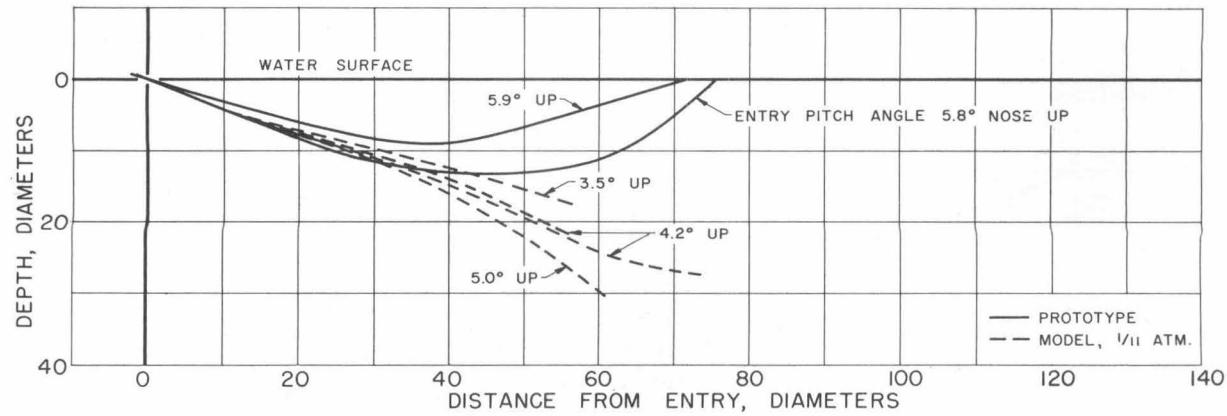

Fig. 4 - Underwater trajectories - Entry pitch angles 3-1/2° to 6° nose up.
Froude scaled model entry velocity: 60 fps.
Prototype entry velocity: 200 fps.
Equal cavitation numbers in model and prototype systems.

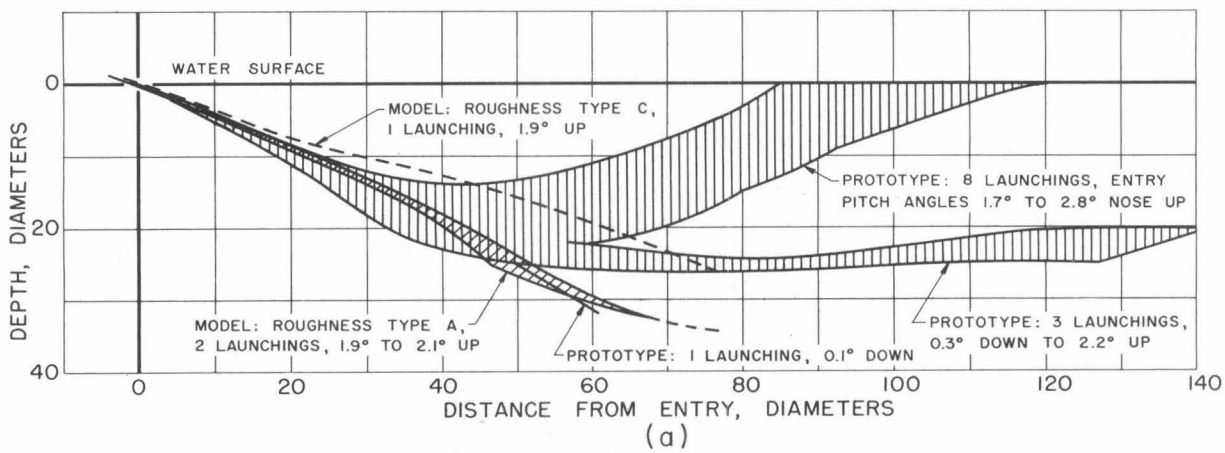

(a)

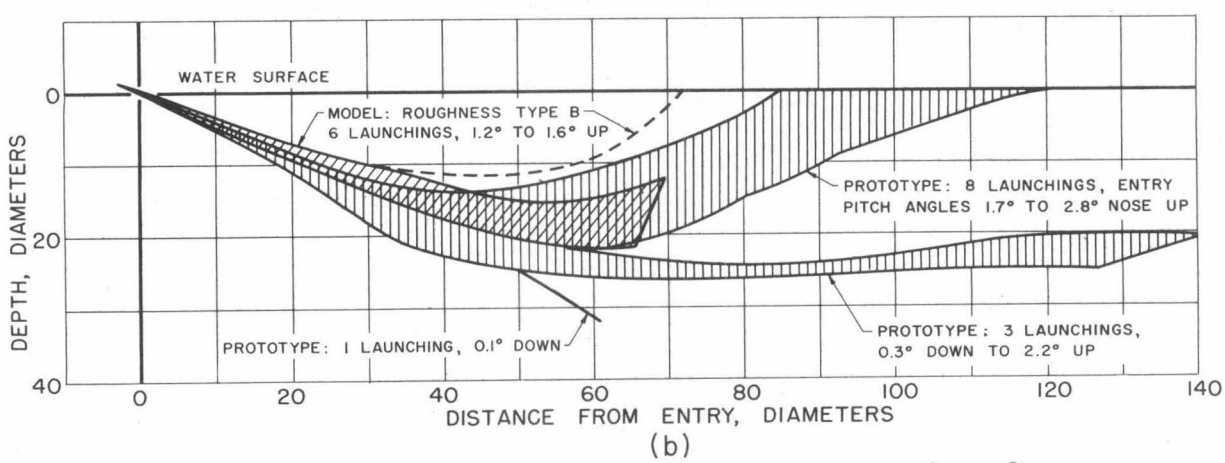

(b)

Fig. 5 - Underwater trajectories - Entry pitch angles 0° to 3° nose up.
Froude scaled model entry velocity: 60 fps.
Prototype entry velocity: 200 fps.
Equal cavitation numbers in model and prototype systems.
Model artificially roughened (Types a, b, and c).

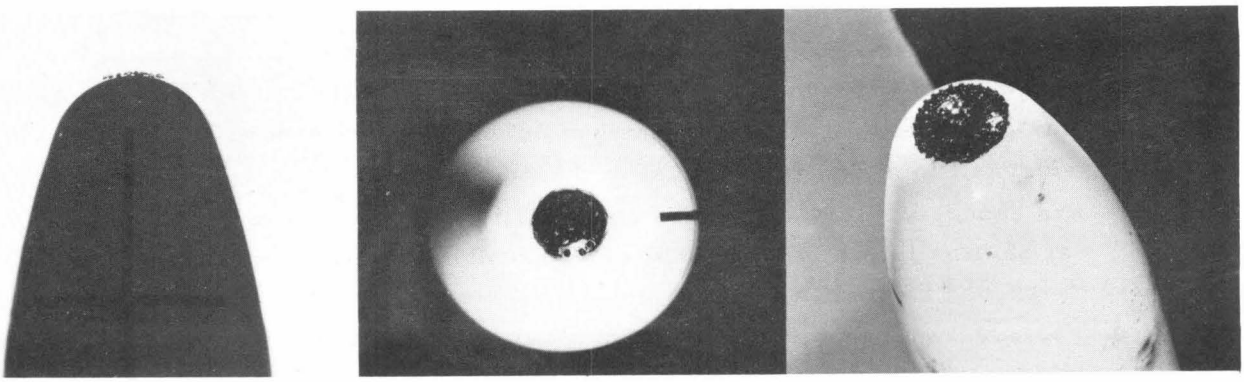

(a) Type A. (b) Type A. (c) Type B.

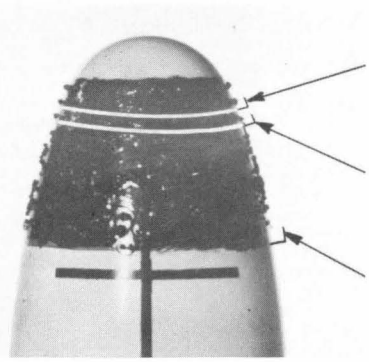

Type C - Two concentric rings of regularly spaced grains of sand on ogival portion of nose.

Type D - Three concentric rings of regularly spaced grains of sand on ogival portion of nose.

Type E - Three concentric rings of regularly spaced grains of sand plus band of sand grains located at random on ogival portion of nose.

(d) Types C, D and E.

Fig. 6 - Model with artificial roughness.

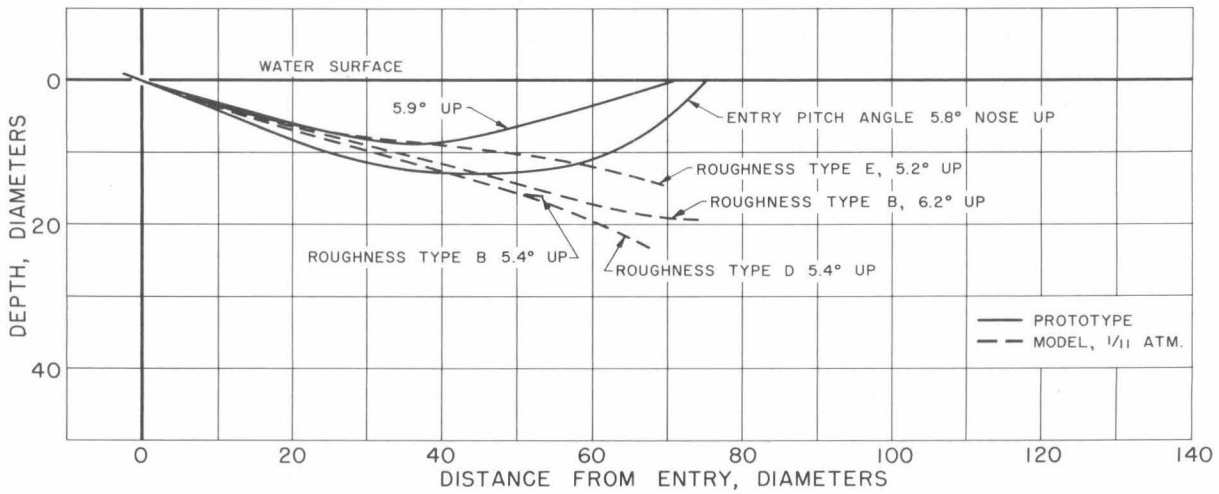

Fig. 7 - Underwater trajectories - Entry pitch angles 4° to 6° nose up.
Froude scaled model entry velocity: 60 fps.
Prototype entry velocity: 200 fps.
Equal cavitation numbers in model and prototype systems.
Model artificially roughened (Types b, d, and e).

to suspect that increasing the drag tends to cause a steeper trajectory. Further tests are planned with entry pitch angles of 4° to 6° nose-up and with entry velocities of 400 fps for the prototype and 120 fps for the model. At an entry velocity of 120 fps a turbulent boundary layer will occur naturally on the model. Hence, the effects of artificial roughness can be eliminated. Effort will also be made to delete or at least make equal the pitch velocities of the model and prototype during the air flight.

Several tests were made with the rough nose model at full atmospheric pressure and 0° entry pitch angle to see if Froude scaling alone would be adequate. The trajectory of the model deviated sharply from that of the prototype when the model remained in its cavity. During half of the number of launchings made, the entry cavity stripped from the model and trailed from the shroud ring after only 1-1/2 or 2 lengths of underwater travel (Fig. 8). To the knowledge of the authors, this cavity stripping has not been observed heretofore. When cavity stripping occurred, the trajectories of the model were comparable to those of the prototype (Fig. 9). Whether the agreement between the trajectories is significant or pure coincidence has not been established, but coincidence is the more likely explanation, as the stripping of the cavity was due, at least in part, to the forces of surface tension.*

During several of the prototype launchings, the inclination of the torpedo with respect to the horizontal was recorded as a function of time. These inclination records were from tests in which the prototype broached within 120 dia. of water entry. Since only one model launching resulted in a broach within that distance, it alone could be compared to the prototype results. This run was made at an air pressure of 1/11 atm. and with roughness of type (b) on the nose tip. The model reproduced the orientation of the prototype as well as its path (Fig. 10).

Tests with Entry Velocities of 400 fps for the Prototype and 120 fps for the Model

Only one prototype launching was made at this entry velocity. Figure 11 shows the trajectory of the prototype compared with the trajectories of the model with both rough (type b) and smooth nose. All of the model tests were made with an air pressure of 1/11 atm. At this velocity the model with both rough and smooth nose reproduced the trajectory of the prototype to within 3 dia. during 70 dia. of underwater travel.

---

*See page 15.

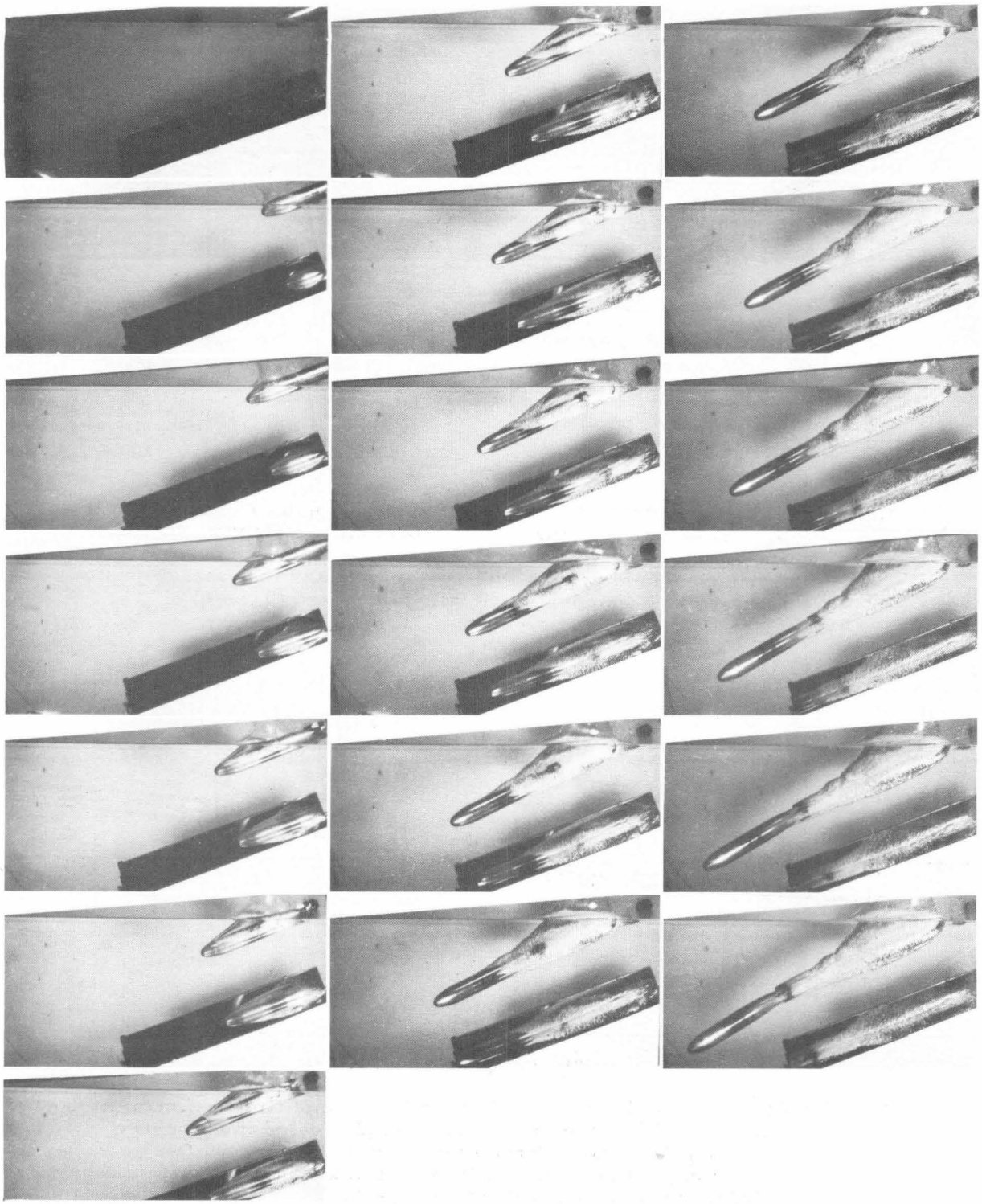

Fig. 8 - Entry cavity stripping from model during first 1-1/2 or 2 lengths of underwater travel. Entry velocity: 60 fps. Air pressure: 1 atm. Model artificially roughened (Type b). Photographed at 400 frames/sec.

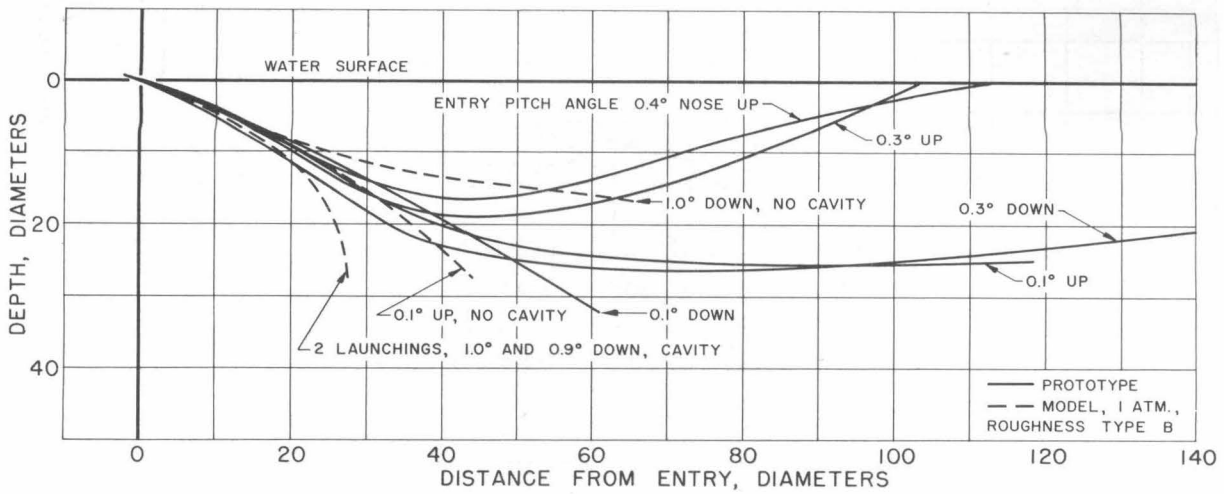

Fig. 9 - Underwater trajectories - Entry pitch angles 1^{o} nose down to 0.4^{o} nose up. Froude scaled model entry velocity: 60 fps. Prototype entry velocity: 200 fps. Cavitation number of model system greater than that of prototype system. Model artificially roughened (Type b).

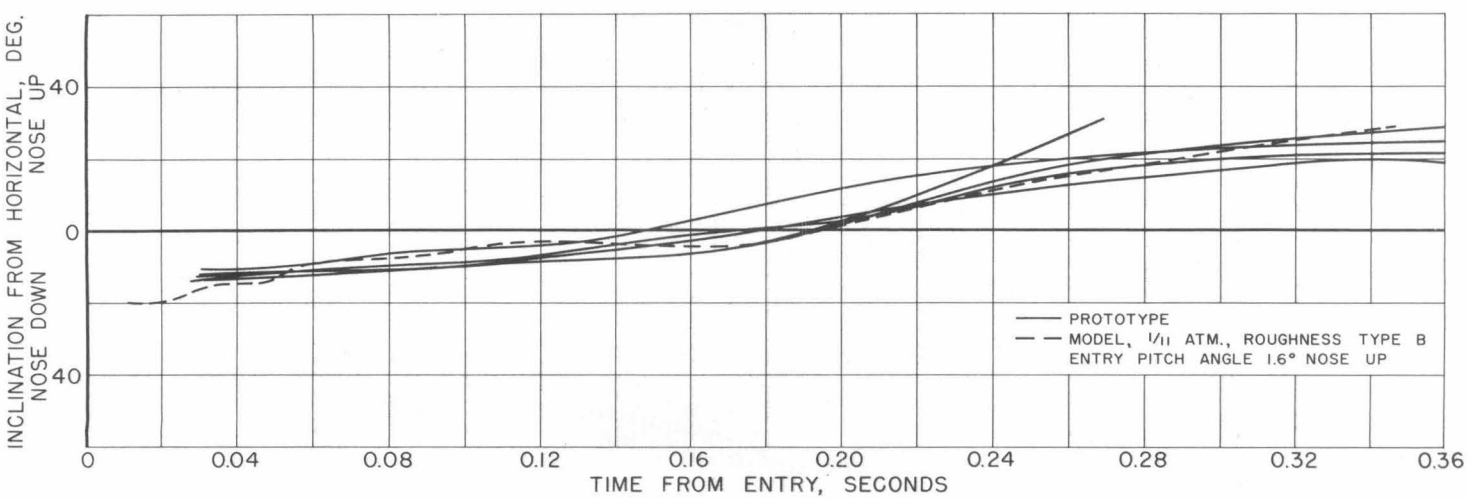

Fig. 10 - Inclination of torpedo axis as a function of time - Entry pitch angles 0.3^{o} to 2.8^{o} nose up. Froude scaled model entry velocity: 60 fps. Prototype entry velocity: 200 fps. Equal cavitation numbers in model and prototype systems. Model artificially roughened (Type b).

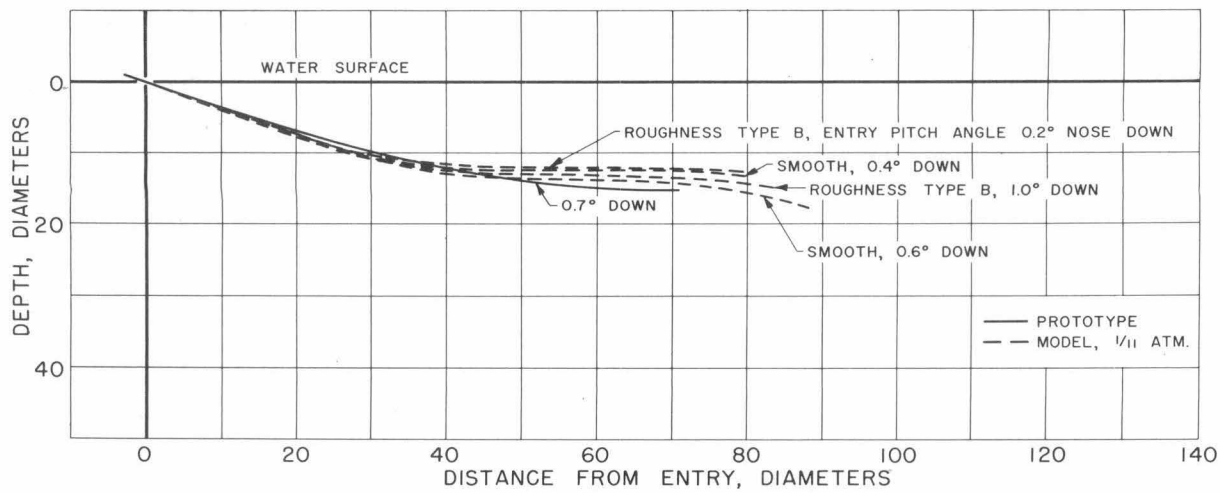

Fig. 11 - Underwater trajectories - Entry pitch angles 0^{o} to 1^{o} nose down.
Froude scaled model entry velocity: 120 fps.
Equal cavitation numbers in model and prototype systems.
Model both smooth and artificially roughened (Type b).

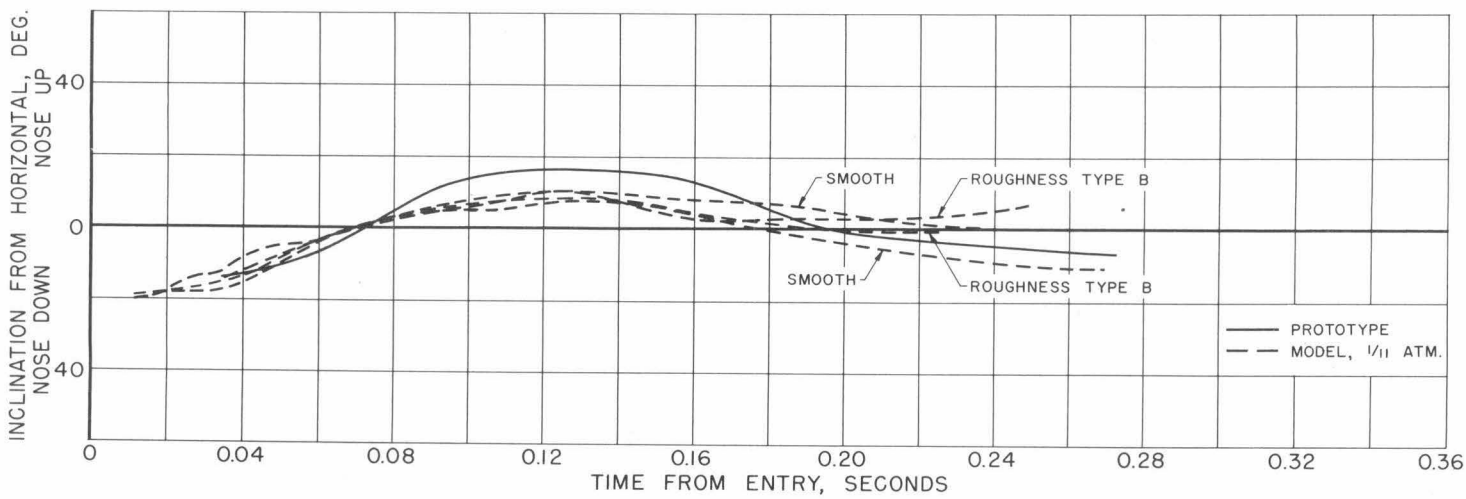

Fig. 12 - Inclination of torpedo axis as a function of time - Entry pitch angles 0^{o} to 1^{o} nose down. Froude scaled model entry velocity: 120 fps. Prototype entry velocity: 400 fps.
Model both smooth and artificially roughened (Type b).

Figure 12 shows the fragmentary inclination record obtained during the prototype test compared with the results from the model launchings. Unfortunately, the beginning of the prototype record was lost, making it impossible to establish zero time. The prototype curve was aligned with the model curves by sliding it horizontally until the first recorded inclination angle equaled the inclination of the model. When this was done, the inclination of the prototype as a function of time differed 6^{o} or less from that of the model during the ensuing 0.27 sec (0.9 sec in the prototype system). The scatter of inclination data for several prototype runs having nearly identical trajectories may be seen in Fig. 10.

When the rough nose model was launched at full atmospheric pressure the model remained in the cavity and the trajectory deviated from that of the prototype, proving that Froude scaling alone was inadequate.

Behavior of the Model

Studying the response of the model to changes in entry conditions and to changes in the physical properties of the model system will be an important phase in modeling so long as it is impossible to observe the behavior of the prototype in detail. Full understanding of the model behavior will lead both to better modeling techniques and to better understanding of the prototype.

Effect of Artificially Induced Turbulent Boundary Layer

There was no large difference in the cavities made by the smooth model and by the model with the various roughnesses (Fig. 13). Detailed photographs of the cavities of the smooth model and of the model with roughness (type b) were taken during launchings with entry velocities of 60 and 80 fps. As long as the cavity did not strip from the roughened model, the roughness made no detectable difference in the cavity at full atmospheric pressure (Fig. 14), but when the air pressure was reduced, the bottom of the cavity made by the smooth model was scalloped and the cavity made by the rough model was not (Fig. 15). The scalloping was probably caused by irregular separation of the flow from the bottom of the model. This could cause the discrepancy between the prototype and the smooth model in the equal cavitation number-Froude scaled system. The scalloping almost disappeared when the velocity of the smooth model was increased to 80 fps (Fig. 16). It was not possible to obtain detailed photographs of launchings with entry velocity of 120 fps where the roughness made no difference in the trajectory, but no indication of scalloping could be detected in the less detailed photographs from the large tank.

The addition of sand to the nose tip (roughnesses a and b) did not affect the drag as long as the model remained in the cavity (Fig. 17). Sand on the

ogival portion of the nose (roughnesses c, d, and e) caused the drag to in increase (Fig. 17). It is interesting that the roughness which caused valid modeling (type b) did not change the drag of the shape. When the model shed its cavity early in the trajectory the drag decreased markedly (Fig. 18).

Early Loss of Entry Cavity

The fact that the roughened model (type b) shed its entry cavity after only 1-1/2 or 2 lengths of underwater travel during several of the full pressure launchings warranted further investigation. A flow having a turbulent boundary layer would be more apt to close about the model than one with a laminar boundary layer. Further, the tendency of the flow to close would increase both as the ambient pressure increased and as the velocity decreased. Therefore, within the scope of this investigation, the loss of the cavity would be most likely to occur with the roughened model at full atmospheric pressure with an entry velocity of 60 fps. In order to establish the conditions under which early loss of the cavity did occur, several launchings were made with entry velocities of 60, 80 and 120 fps. The model with the smooth nose could not be made to leave its cavity, nor did the roughened model leave the cavity when launched at an air pressure of 1/11 atm. Fifteen launchings were made with the roughened model at full atmospheric pressure, eight at 60 fps, four at 80 fps, and three at 120 fps. At 60 and 80 fps the cavity stripped during half of the launchings; at 120 fps the cavity did not strip at all.

Reducing Surface Tension of Water Prevents Early Loss of Cavity

Simultaneous modeling by both Froude and Weber* criteria requires that the surface tension of the liquid in the model system be less than 1/100 that of the prototype. It has previously been considered unnecessary to model surface tension at entry velocities as high as 60 fps. However, in an attempt to explain the stripping of the entry cavity the surface tension of the liquid in the small tank was reduced from 76 to 40 dynes/cm by adding aerosol (solution concentration less than 0.1% aerosol by weight). This reduction in surface tension obviously is insufficient to constitute modeling. Four launchings with an entry velocity of 60 fps and at full atmospheric pressure were made into the dilute solution of aerosol. The cavity did not strip, indicating that surface tension forces at least in part cause the phenomenon. Figure 19 compares the entry cavities made by the model in water with one in the aerosol solution. There is very little difference between the cavity in the low surface tension liquid and the water cavity that did not strip from the model.

$$*W = \frac{v}{\sqrt{\sigma/\rho\ell}} \qquad \frac{\text{inertia forces}}{\text{surface tension forces}}$$

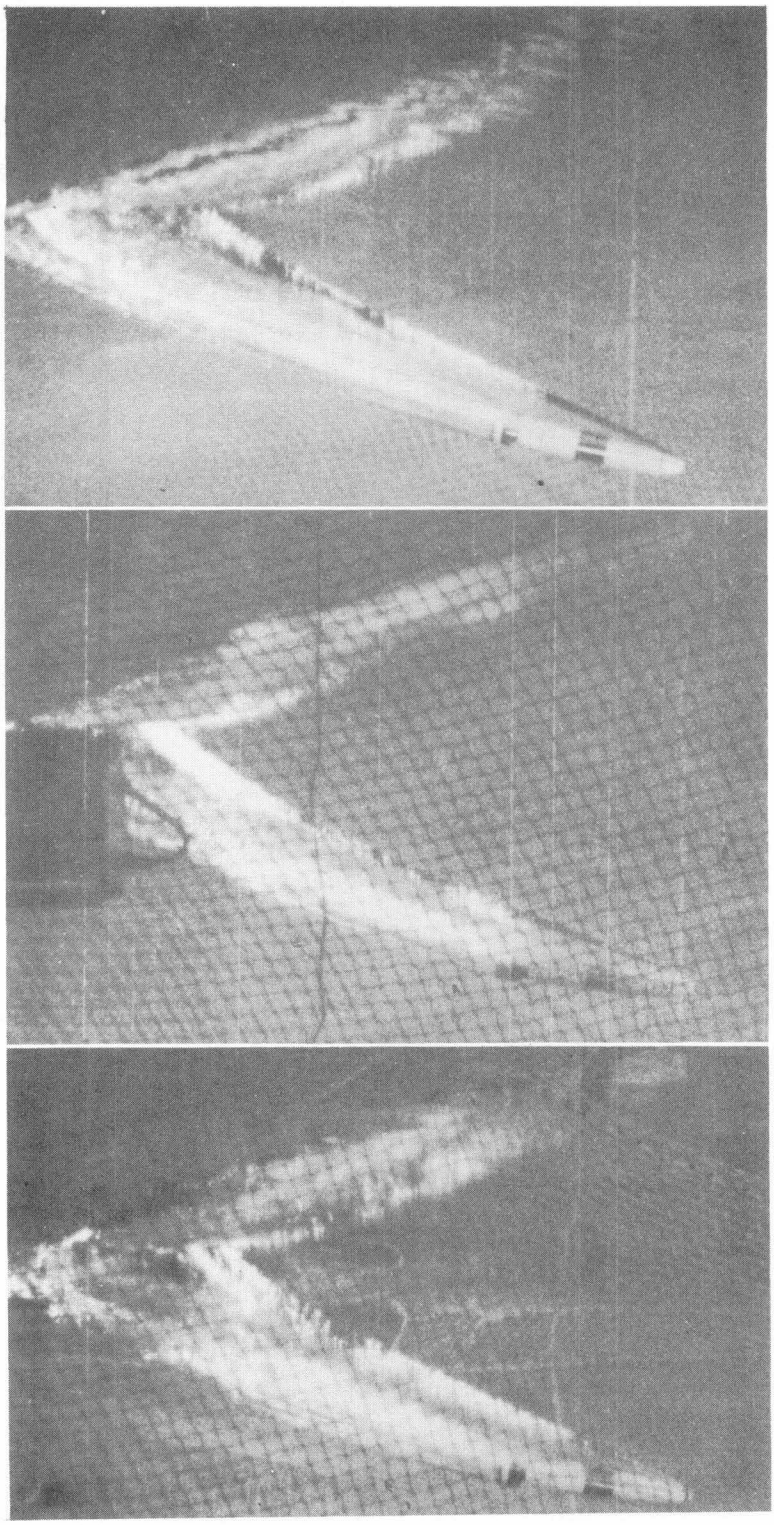

(a) Smooth model.

(b) Artificial roughness (Type b) on nose tip.

(c) Artificial roughness (Type c) on ogive.

Fig. 13 - Entry cavities approximately 80 milliseconds after water entry. Entry velocity: 60 fps.

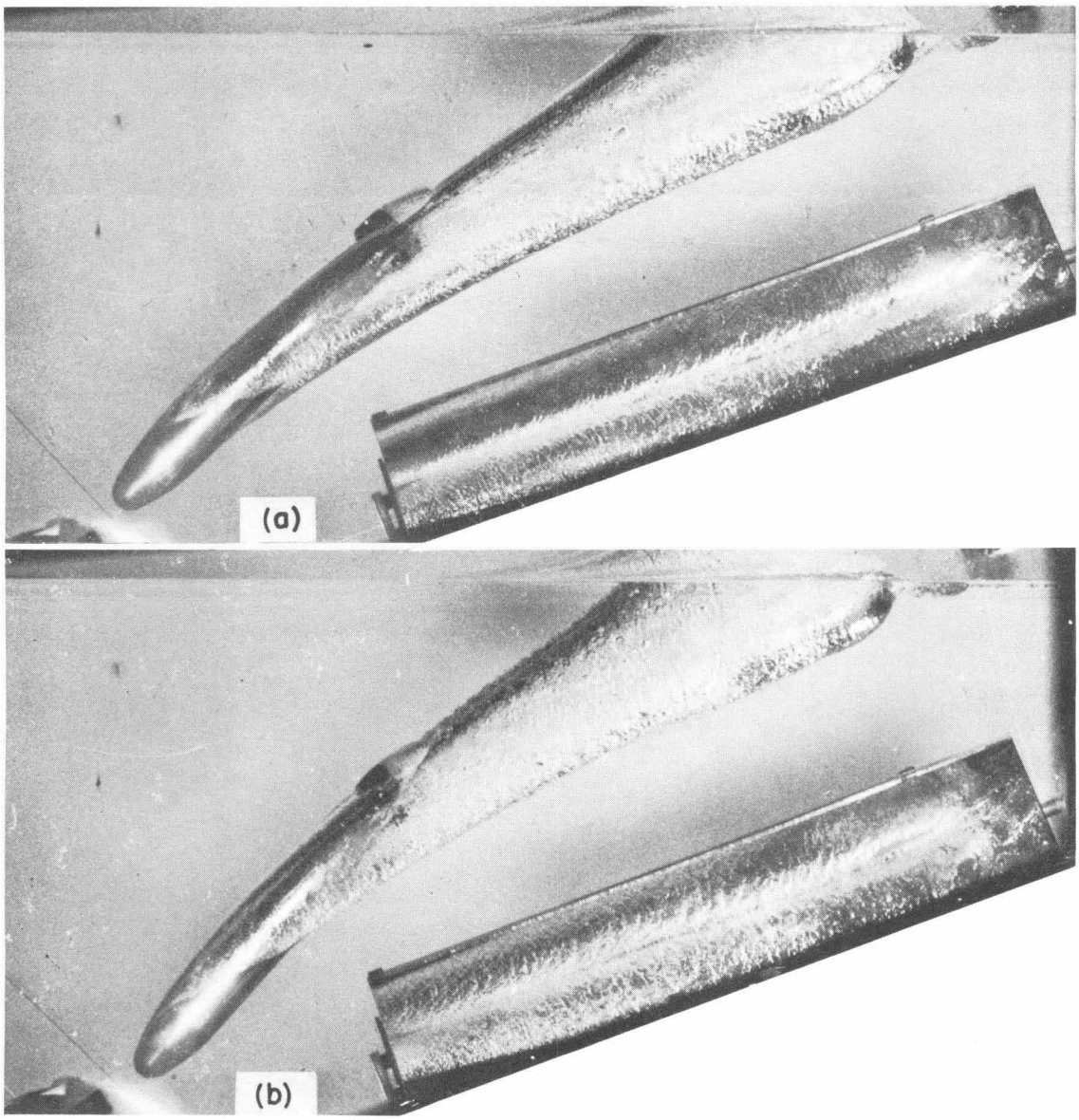

Fig. 14 - Entry cavities 47 milliseconds after water entry.
Entry velocity: 60 fps. Air pressure: 1 atm.

(a) Smooth model. (b) Model with artificial roughness (Type b) on nose tip.

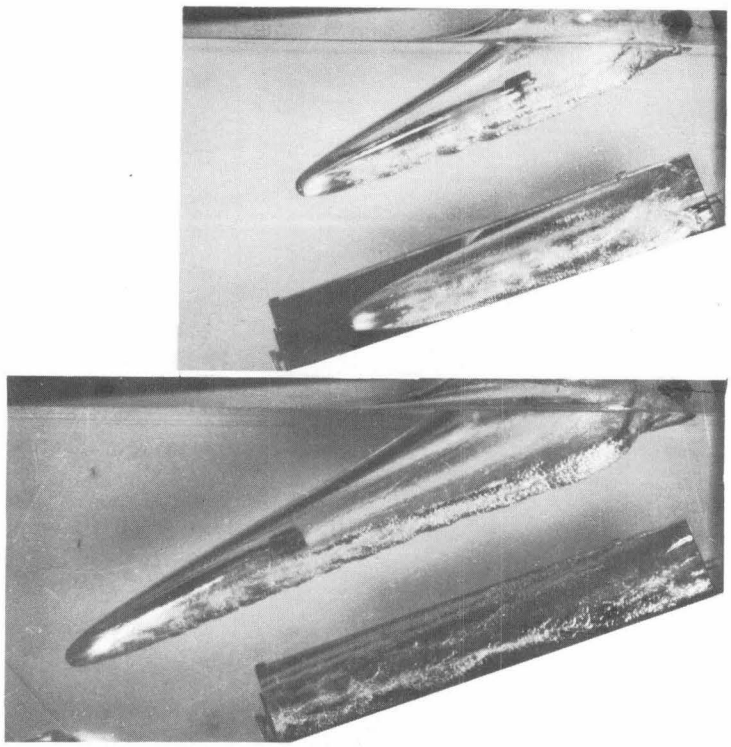

(a) Smooth model.

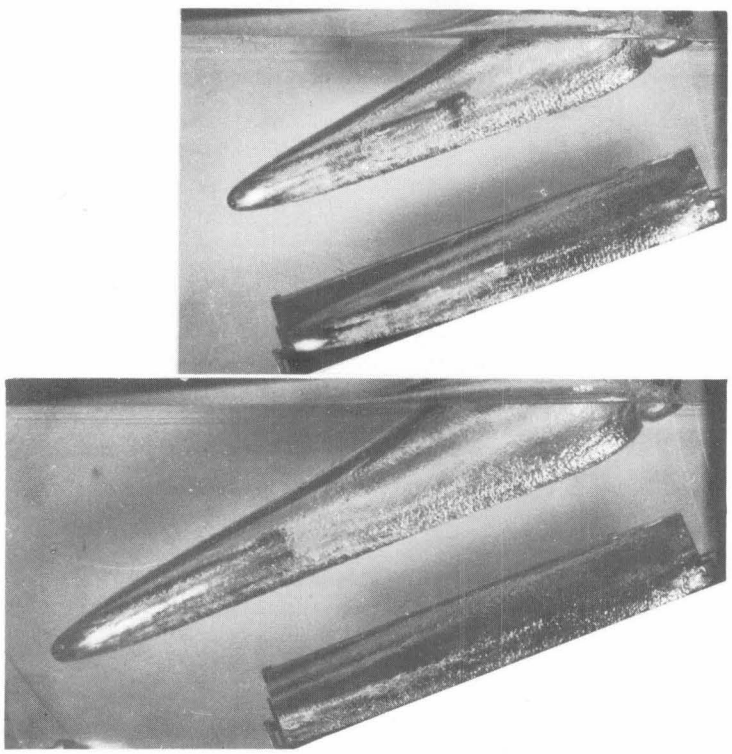

(b) Model with artificial roughness (Type b) on nose tip.

Fig. 15 - Entry cavities 32 and 47 milliseconds after water entry.
Entry velocity: 60 fps. Air pressure: 1/11 atm.

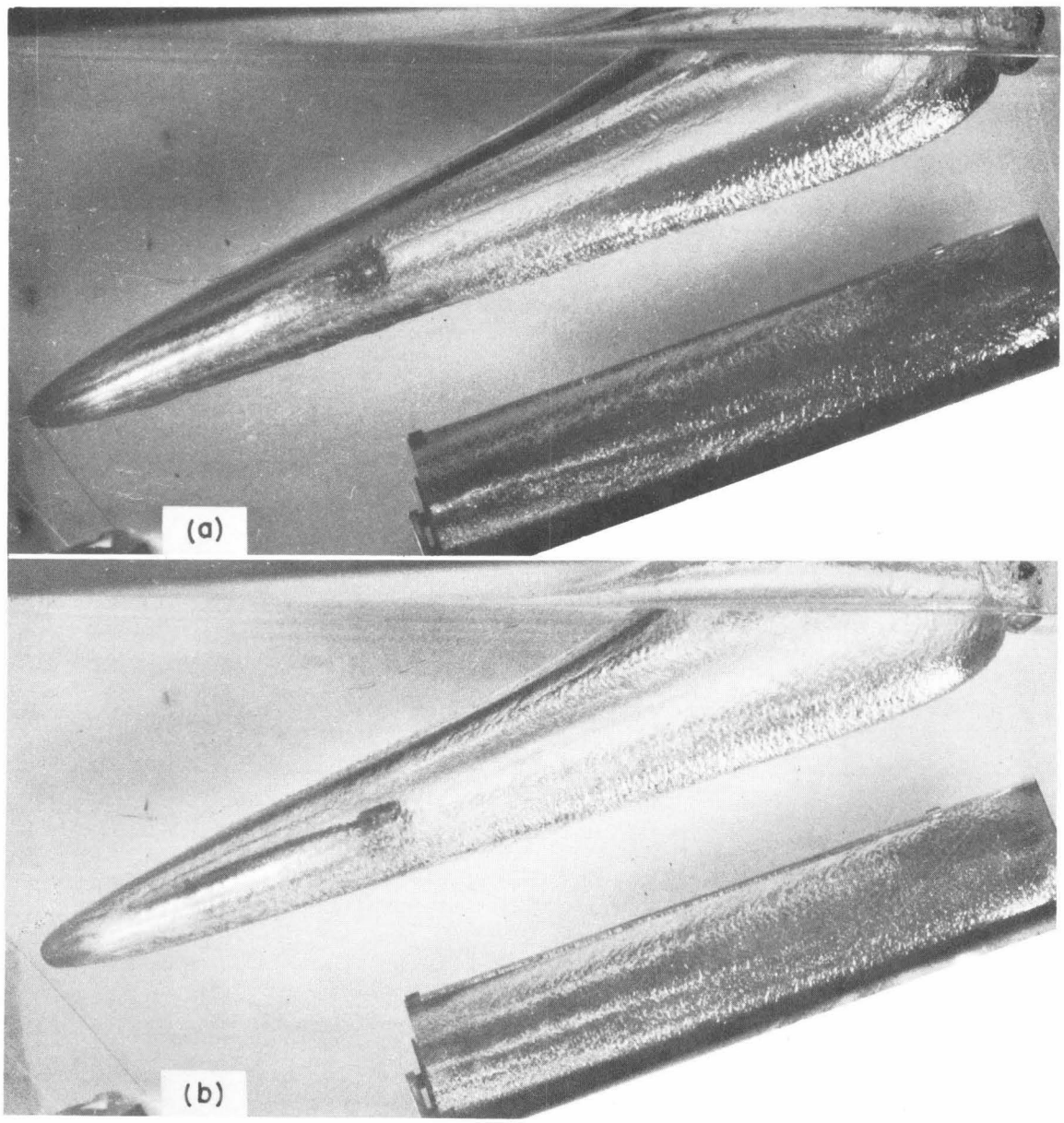

Fig. 16 - Entry cavities 38 milliseconds after water entry.
Entry velocity: 80 fps. Air pressure: 1/11 atm.

(a) Smooth model.

(b) Model with artificial roughness (Type b) on nose tip.

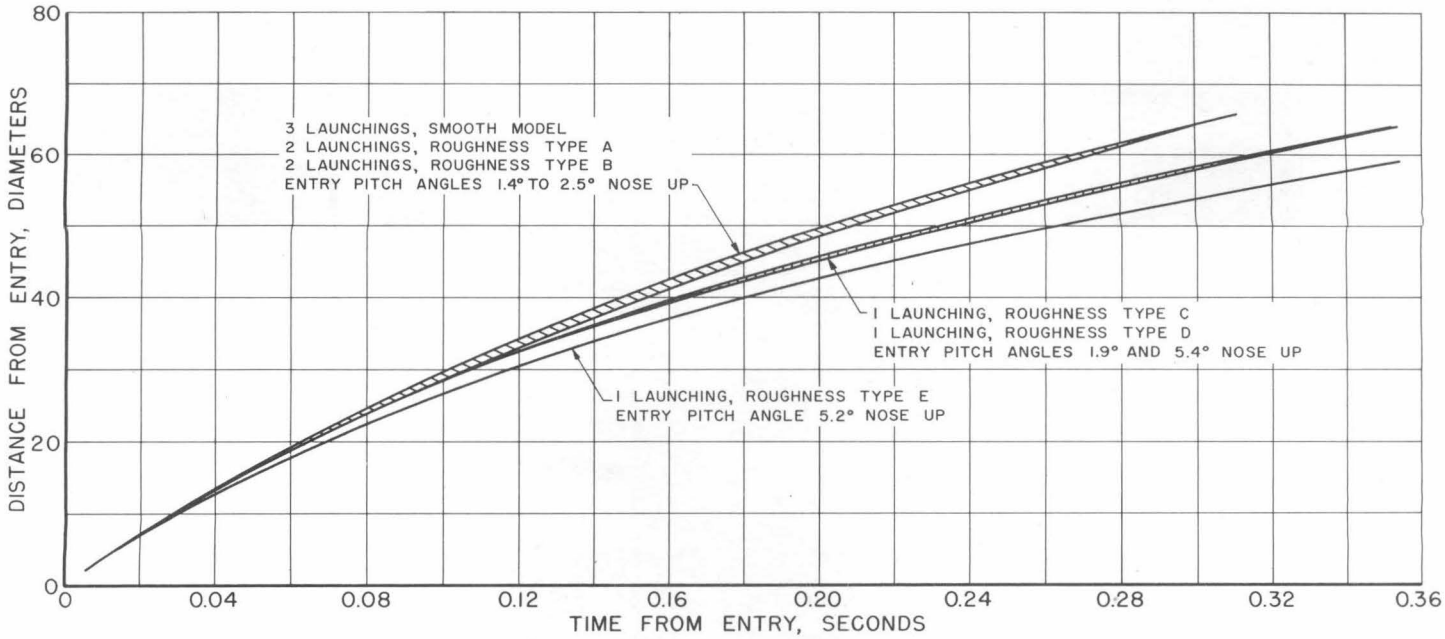

Fig. 17 - Distance from water entry as a function of time. Entry velocity: 60 fps. Air pressure: 1/11 atm. Model smooth and with artificial roughnesses (Types a through e).

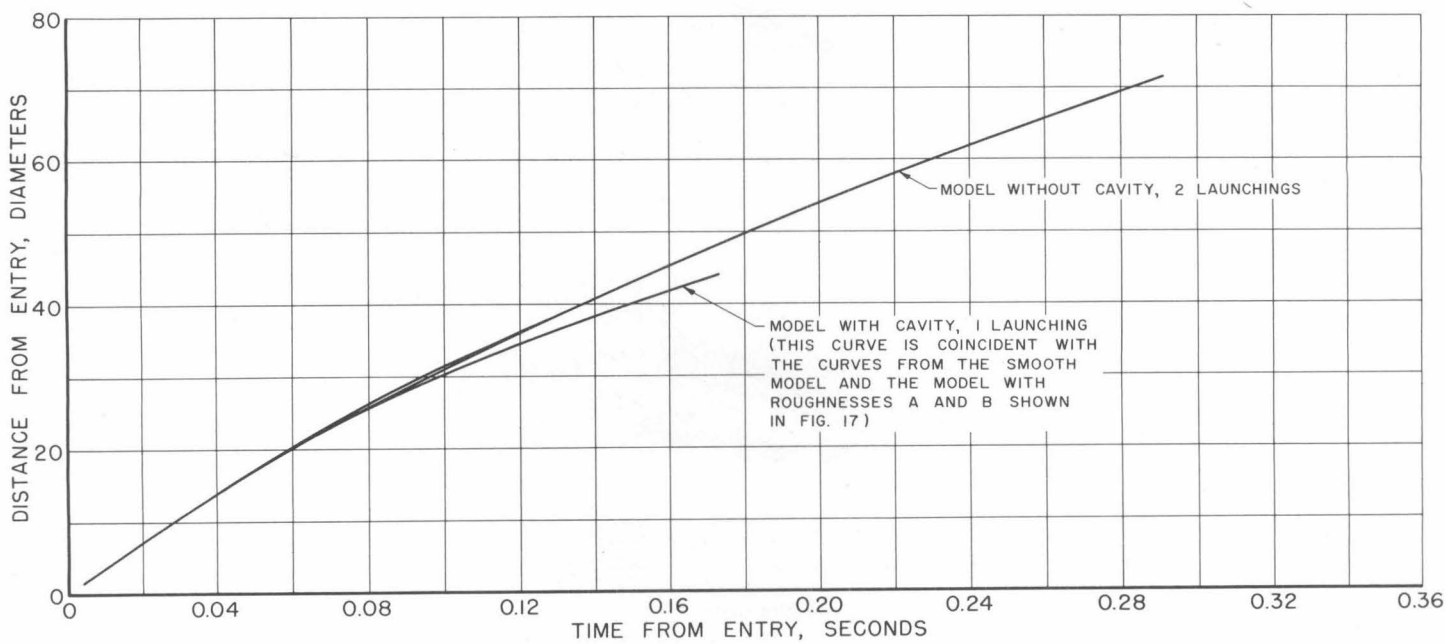

Fig. 18 - Distance from water entry as a function of time. Entry velocity: 60 fps. Air pressure: 1 atm. Model smooth and with artificial roughness (Type b) on nose tip.

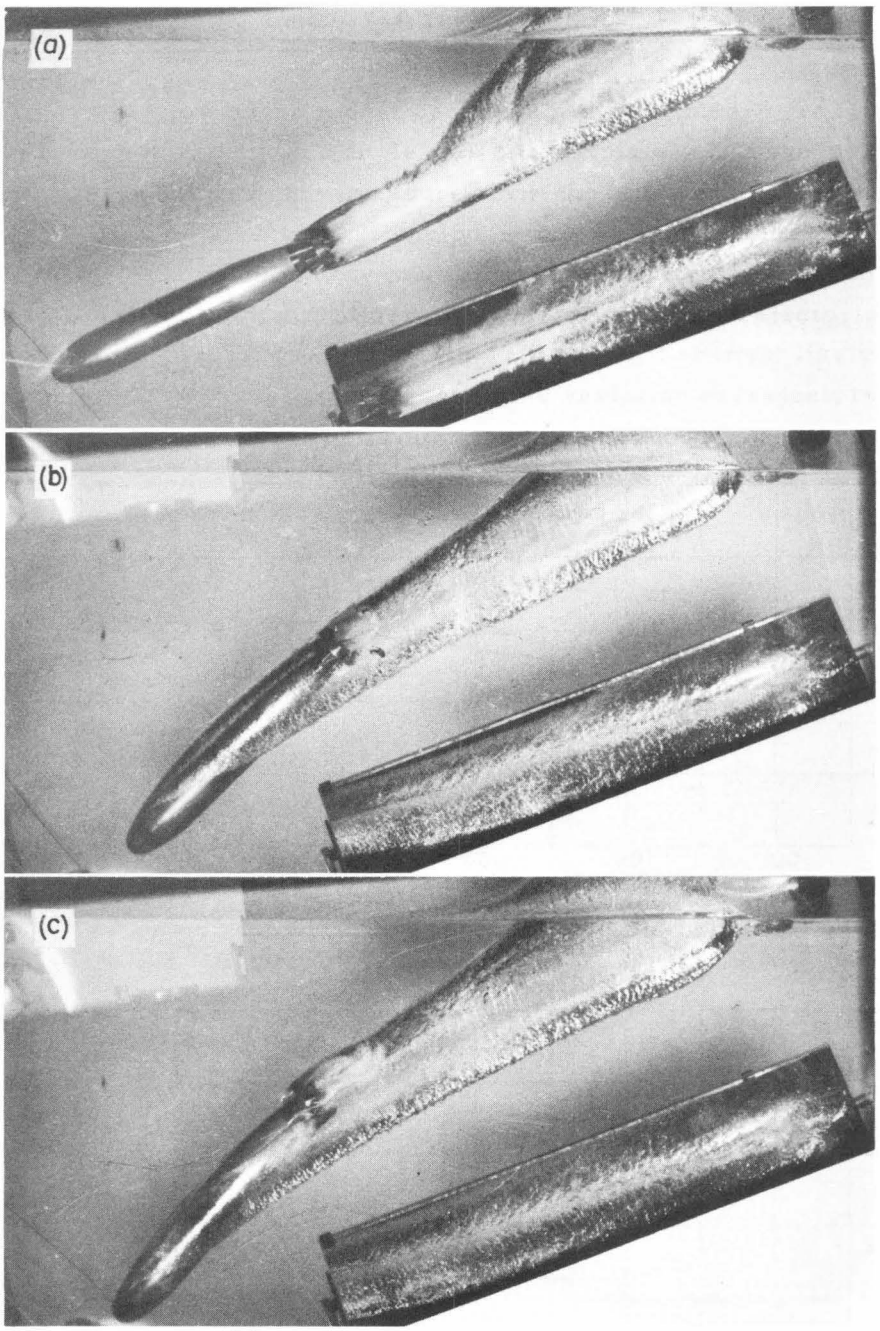

Fig. 19 - Entry cavities 47 milliseconds after water entry.
Entry velocity: 60 fps. Air pressure: 1 atm.
Model with artificial roughness (Type b) on nose tip.

(a) Surface tension of water: 76 dynes/cm.

(b) Surface tension of water: 76 dynes/cm.

(c) Surface tension of dilute aerosol solution: 40 dynes/cm.

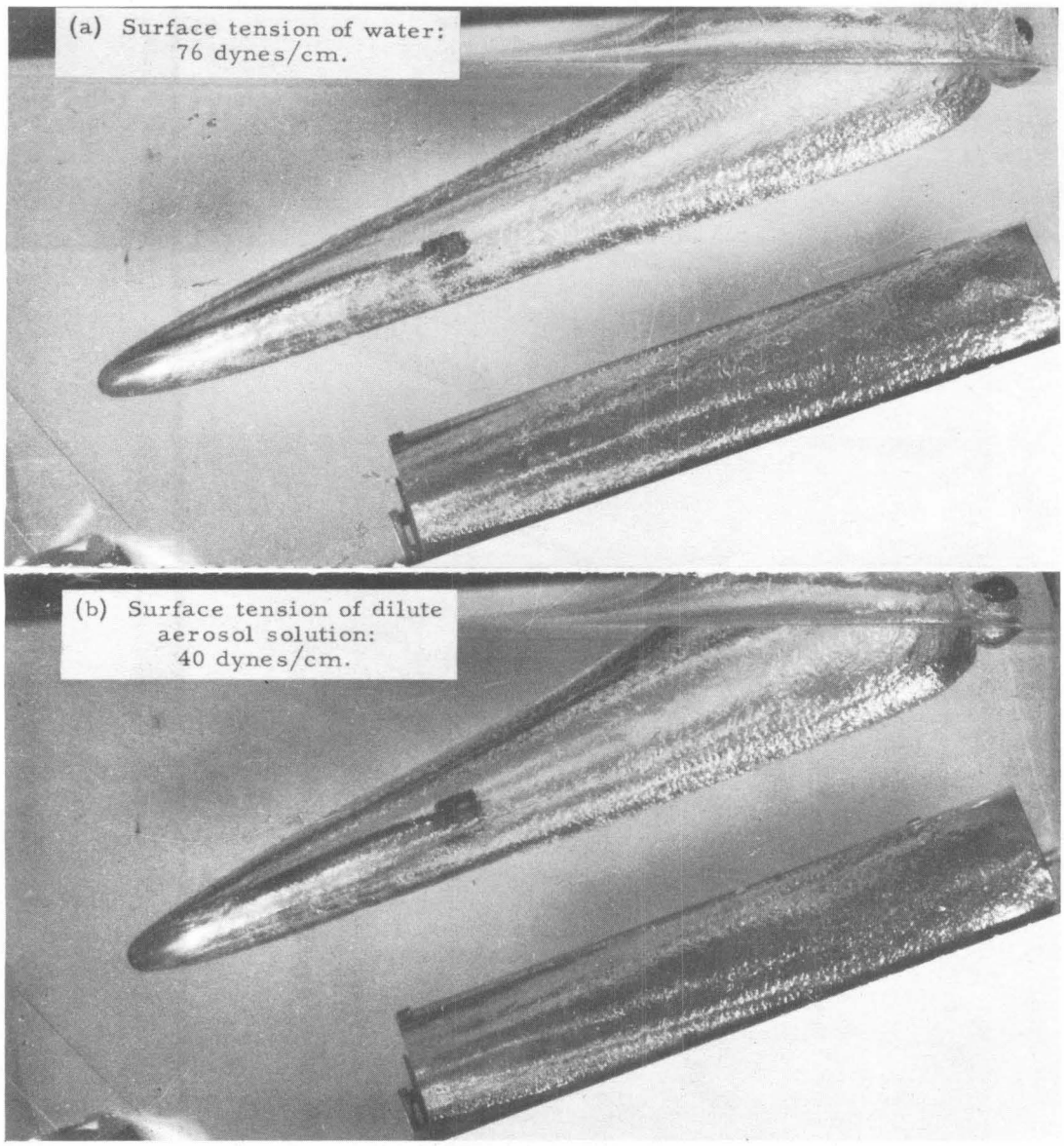

Fig. 20 - Entry cavities 45 milliseconds after water entry.
Entry velocity: 60 fps.
Air pressure in model system: 1/11 atm.
Model with artificial roughness (Type b) on nose tip.

One launching was made into the aerosol solution with the air pressure reduced at 1/11 atm. The shape of the cavity at reduced pressure was unaltered by change in surface tension (Fig. 20). Since the cavity did not strip when the air pressure was reduced, it was not necessary to consider surface tension in the equal cavitation-Froude scaled system. However, since surface tension did make a difference at full atmospheric pressure, it is well to remember that it might be important in modeling other shapes or in modeling the 3-1/2-cal. 70° spherogive under other entry conditions.

The Effect of Entry Pitch Angle

At the trajectory angle used in these tests the spherical portion of the nose contacts the water first if the initial pitch is steeper than 0^{o} to 1^{o} nose down; if the pitch is flatter than 3^{o} or 4^{o} nose up, the ogive contacts first. In the intermediate pitch range the contact is at the junction between sphere and ogive. At an air pressure of 1/11 atm. the shape initially contacting the water appears to influence the trajectory of the model (Fig. 21). The data taken at full atmospheric pressure are insufficient to show whether a similar trend exists (Fig. 22).

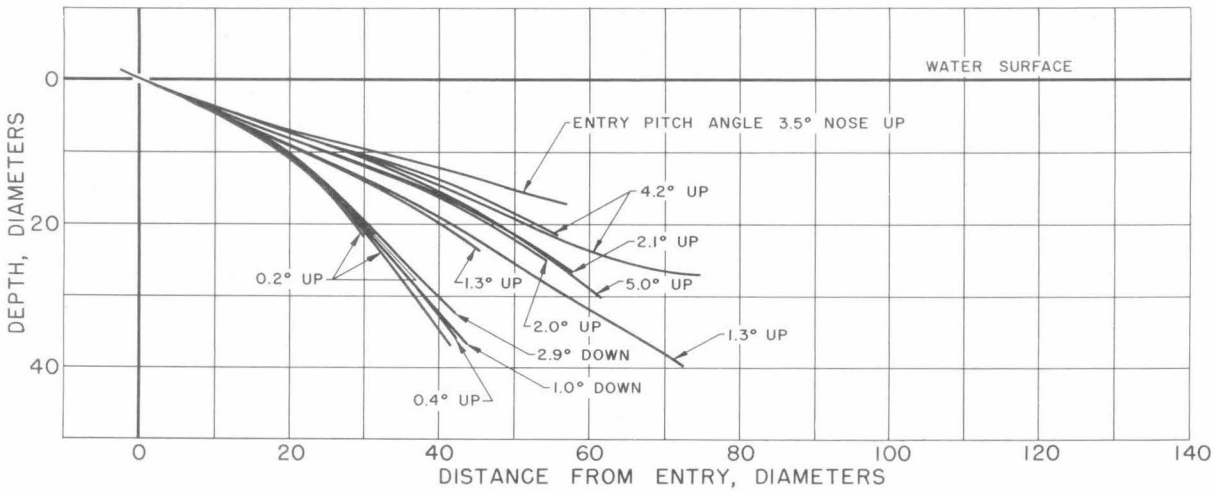

Fig. 21 - Underwater trajectories of smooth model - Entry pitch angles 3^{o} nose down to 5^{o} nose up.
Entry velocity: 60 fps. Air pressure: 1/11 atm.

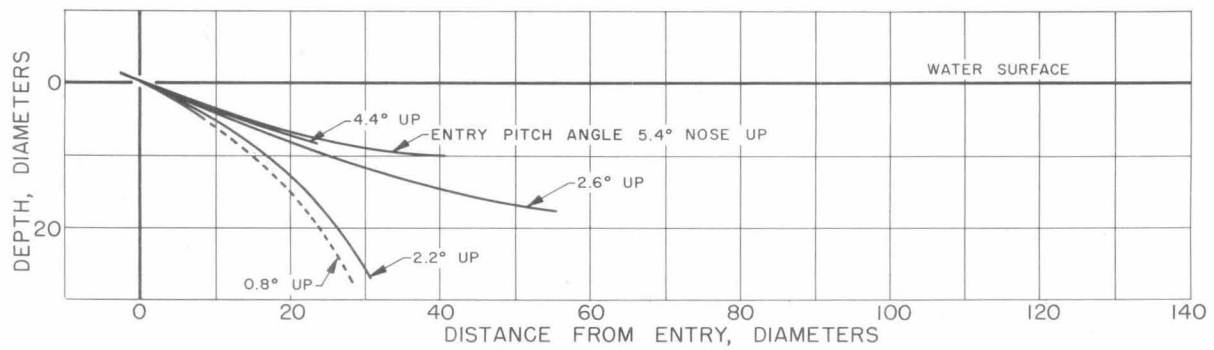

Fig. 22 - Underwater trajectories of smooth model - Entry pitch angles 0.8^{o} to 5.4^{o} nose up.
Entry velocity: 60 fps. Air pressure: 1 atm.

The change in the velocity of the model, as a function of time, was not significantly altered by change in entry pitch angle (Fig. 23), indicating that the orientation of the model in the cavity and the degree of contact between the model and the water had little effect upon the drag.

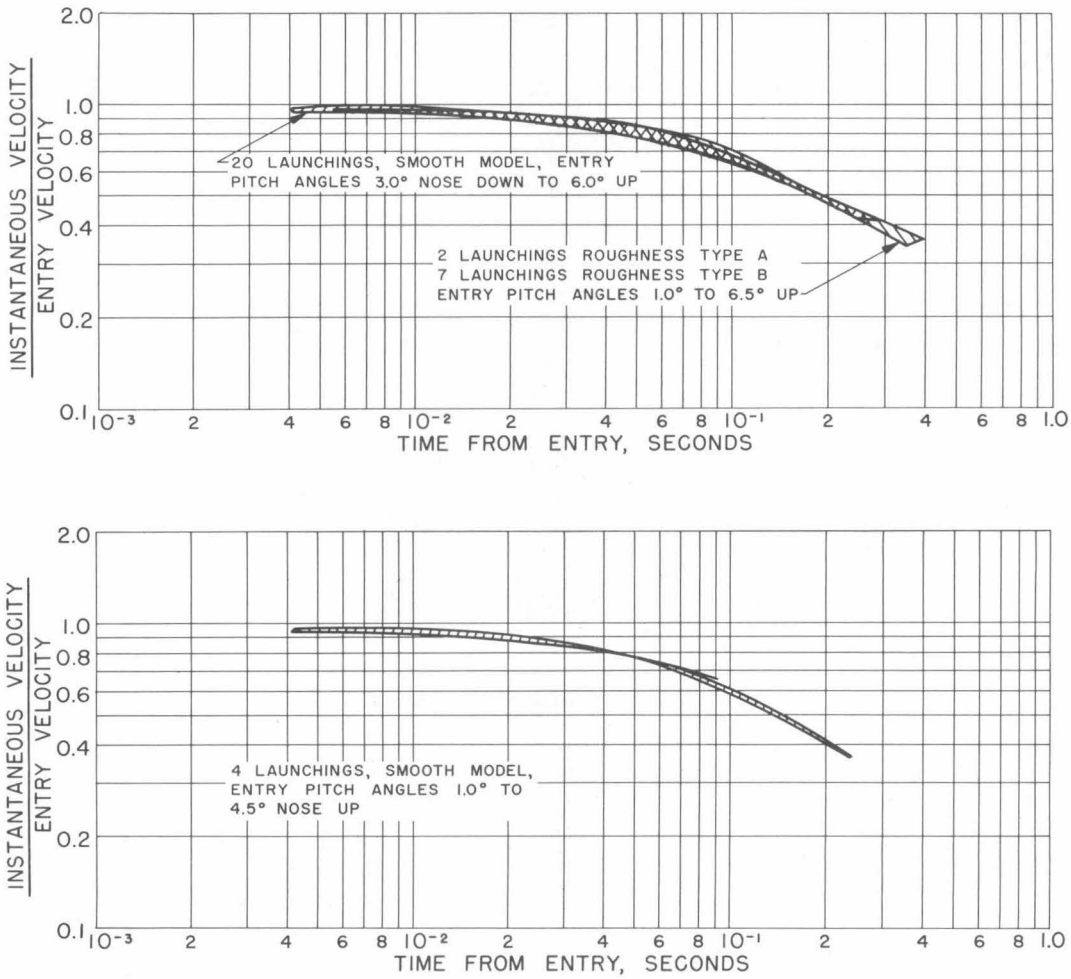

Fig. 23 - The ratio of instantaneous velocity to entry velocity as a function of time. Entry velocity of model: 60 fps.

(a) Air pressure: 1/11 atm.

(b) Air pressure: 1 atm.

Effect of Air Pressure in the Model System

The trajectory of the model became flatter as the air pressure was decreased when the entry pitch angle was approximately 2^{o} nose up and became steeper with decrease in air pressure when the entry pitch angle was from 4^{o} to 6^{o} nose up (Fig. 24). Figure 25 includes photographs of four typical launchings from Fig. 24. The entry cavity and the orientation of the model in Series b, c, and d are originally quite similar. Why the subsequent trajectories should be different is not obvious from the photographs, but it is most likely that differences in separation from the nose cause the variation in trajectory. Unfortunately, the lines of separation around the nose cannot be detected in Fig. 25.

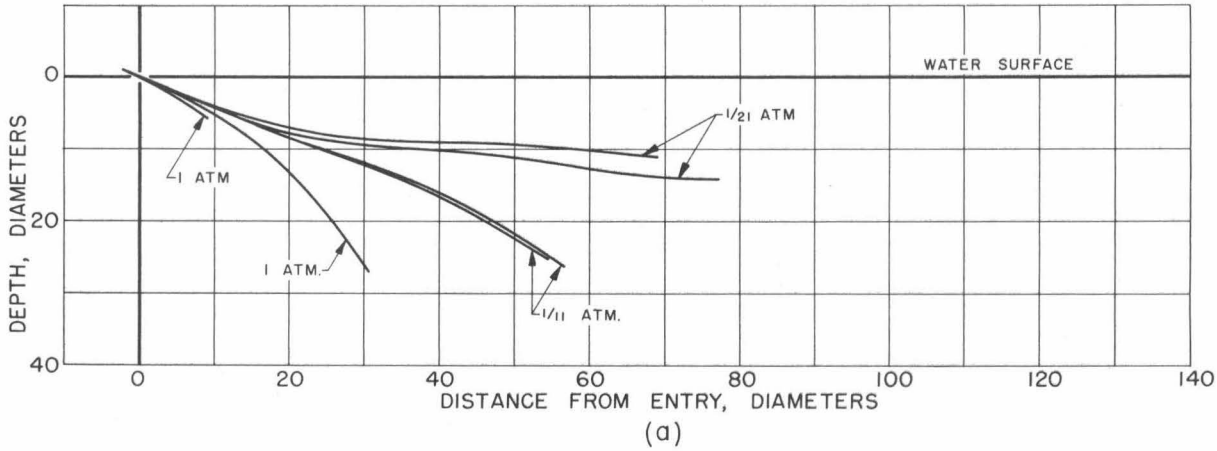

(a)

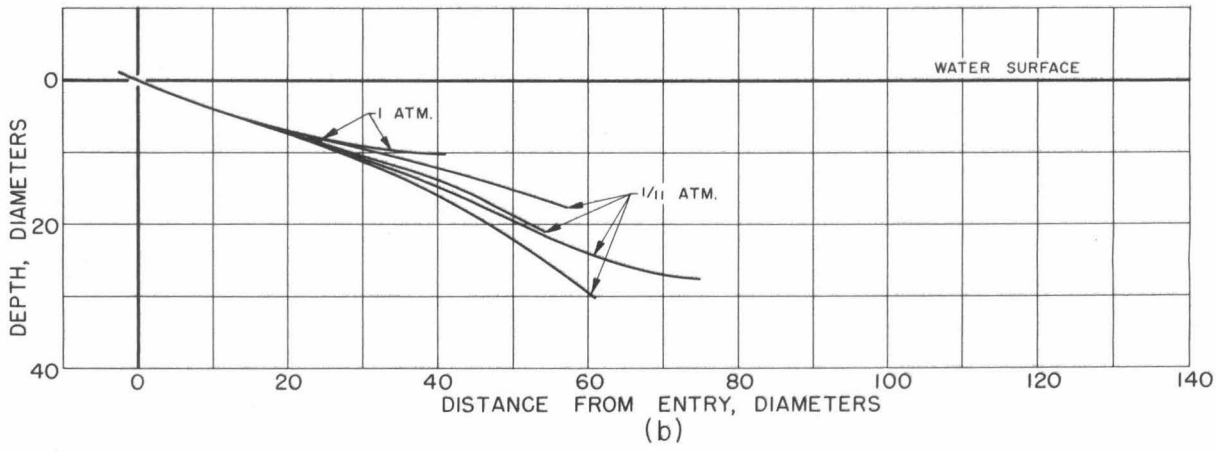

(b)

Fig. 24 - Underwater trajectories of smooth model - Entry velocity: 60 fps
(a) Entry pitch angles - 1^{o} to 2.5^{o} nose up.
(b) Entry pitch angles - 4^{o} to 6^{o} nose up.

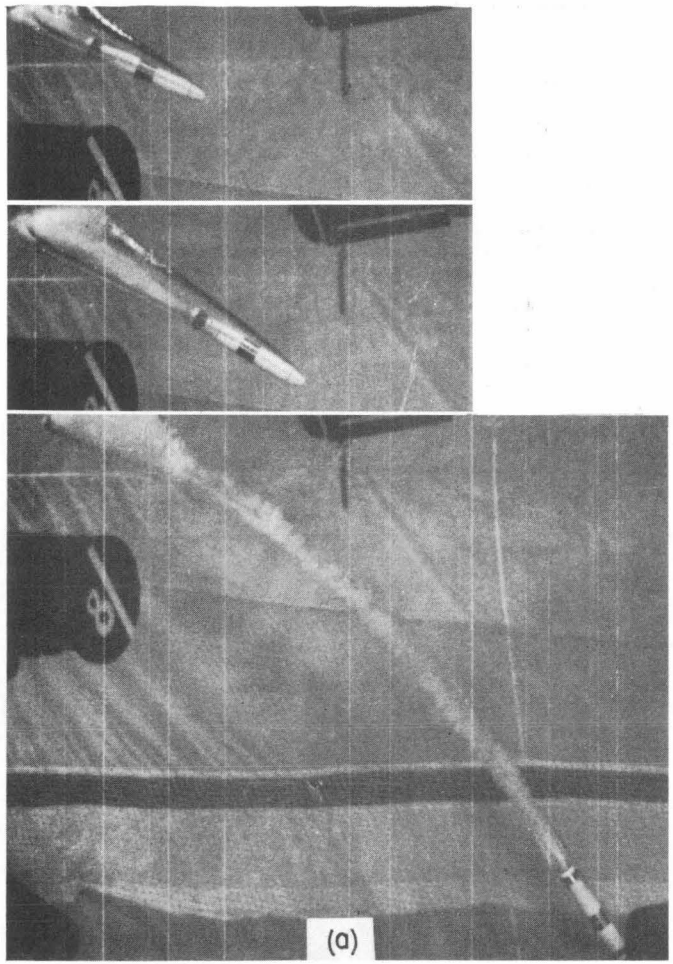

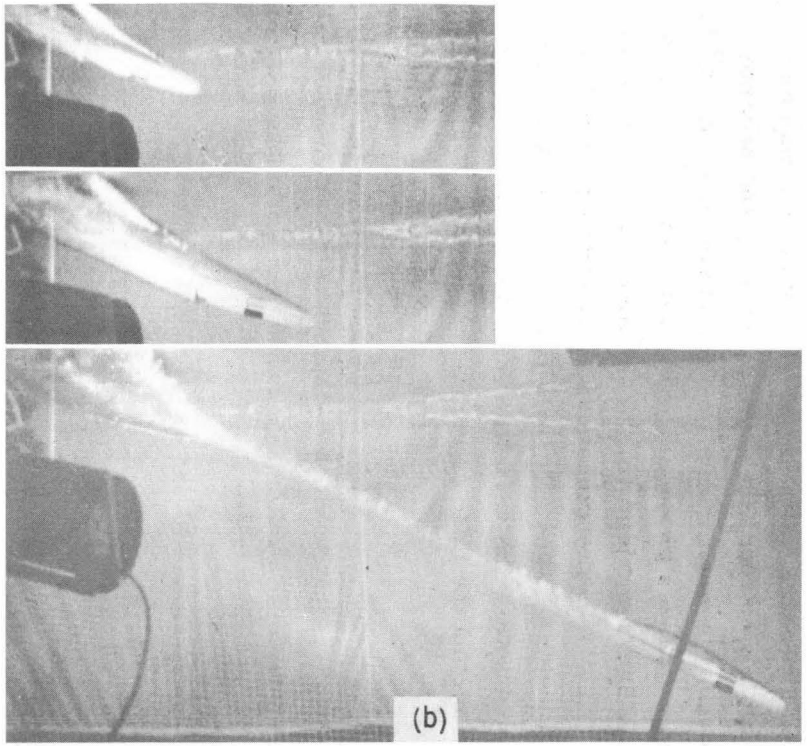

(a) Air pressure: 1 atm.
Entry pitch angle: 2.2° nose up.

(b) Air pressure: 1/11 atm.
Entry pitch angle: 2.5° nose up.

Fig. 25 - Smooth model and entry cavity
31, 52 and 167 milliseconds
after water entry.

CONFIDENTIAL

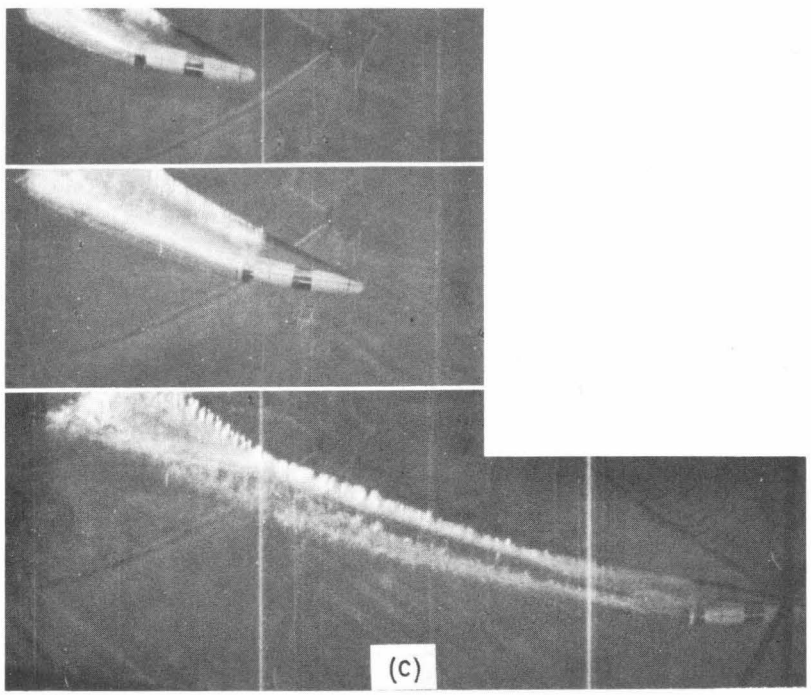

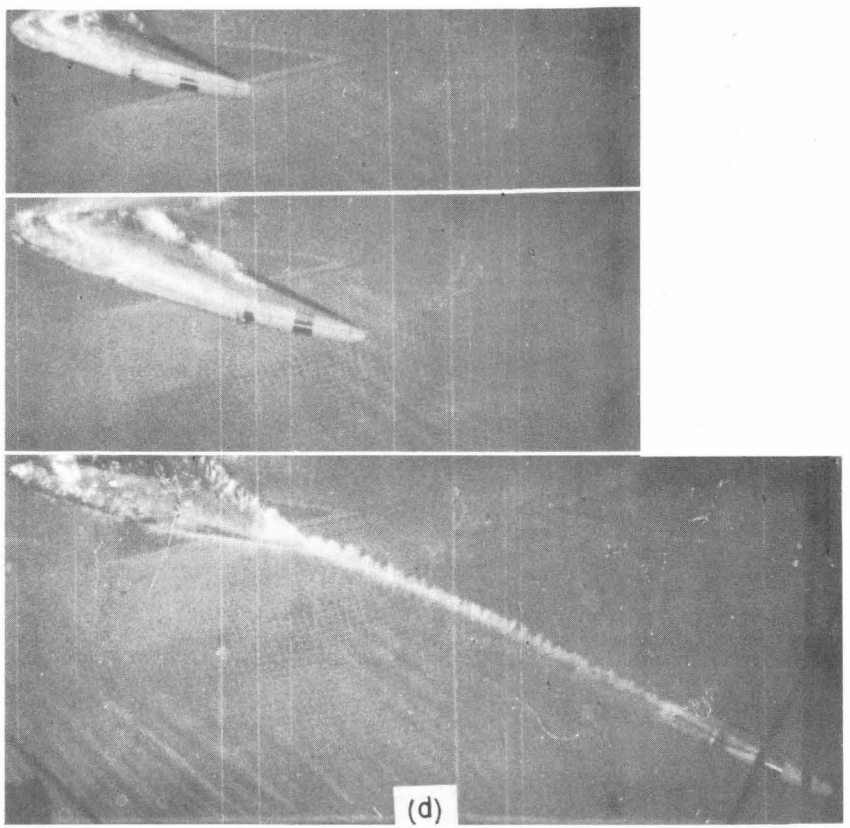

(c) Air pressure: 1 atm.
Entry pitch angle: 5.4° nose up.

(d) Air pressure: 1/11 atm.
Entry pitch angle: 5.0° nose up.

Fig. 25 - Smooth model and entry cavity
31, 52 and 167 milliseconds
after water entry.

CONFIDENTIAL

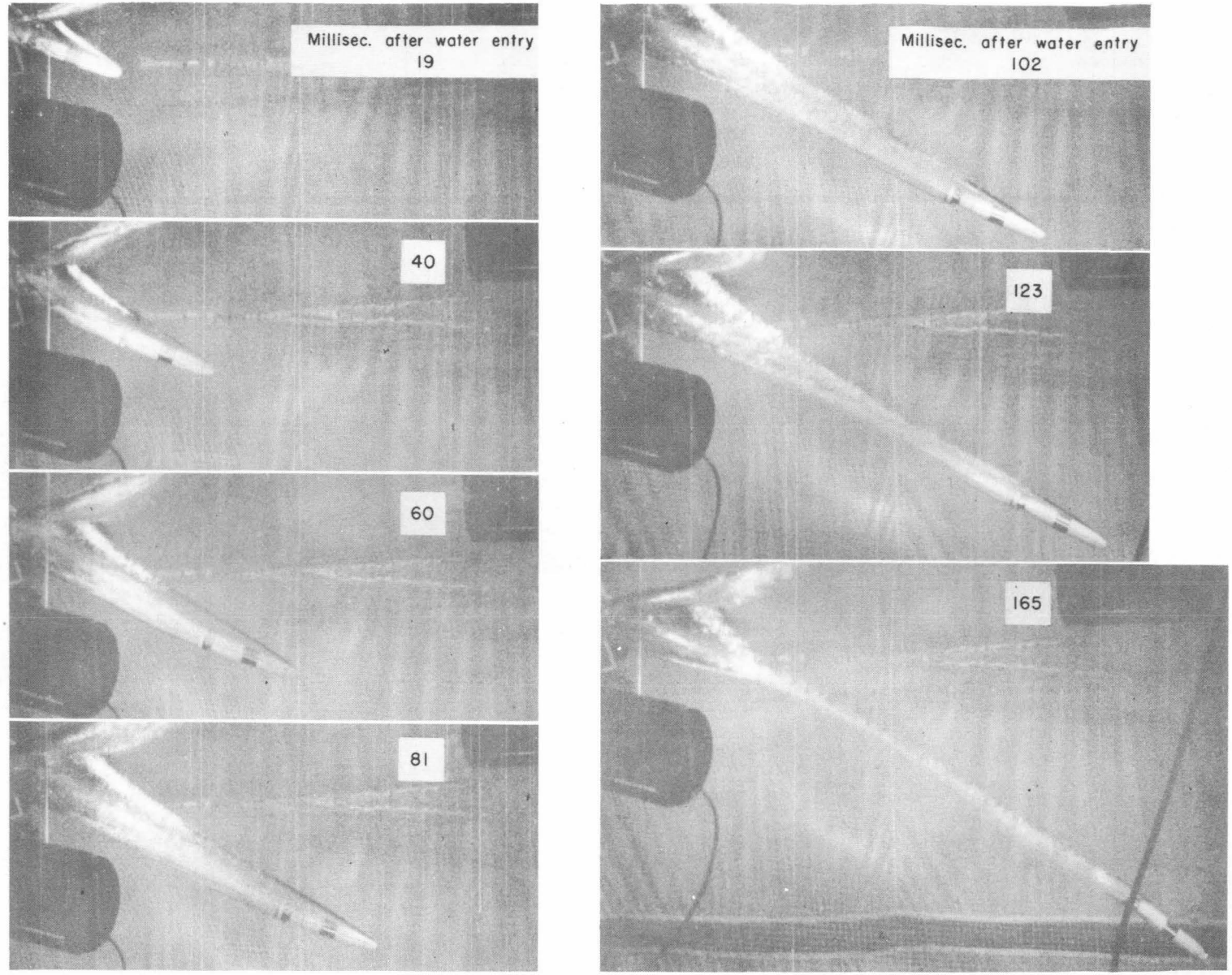

Fig. 26 - Smooth model and entry cavity - Entry velocity: 60 fps.
Air pressure: 1/11 atm. Entry pitch angle: 1.4° nose up.

However, the forces on the nose of this model do appear to be more important than the forces on the tail, because in many instances the contact of the tail with the bottom of the cavity was not sufficient to prevent a downturning trajectory (Fig. 26). Furthermore, the deceleration of the model was almost the same whether the tail initially contacted the water at entry or 70 milliseconds later (Fig. 27). Past investigations have shown that the drag of the Mk 13-6 torpedo increased noticeably when the tail contacted the cavity wall.[9]

The air pressure in the model system also made little difference in the velocity-time function (Fig. 28). The curves from 1 and 1/11 atm. are the average of the individual tests shown in Fig. 23. The results from the two launchings made at 1/21 atm. are also included in Fig. 28.

Effect of Entry Velocity

Increasing the entry velocity flattened the trajectory (Fig. 29). The deceleration of the model was also affected by change in the velocity. The average drag coefficient during the first 26 dia. of underwater travel was 0.17 for an entry velocity of 60 fps and 0.12 for an entry velocity of 120 fps. This value of 0.12 is in good agreement with the value of 0.11 measured for the prototype (entry velocity of 400 fps) during the first length of underwater travel.[8]

CONCLUSIONS

The following conclusions may be drawn from this series of tests made with the Mk 25 torpedo shape with 3-1/2-cal. 70° spherogive head.

A. Comparison of Model and Prototype

1. The equal cavitation number Froude scaling is sufficient to reproduce the trajectory of the prototype and its attitude in space if the velocity of the model is great enough to cause a turbulent boundary layer in the flow.

2. It is possible to induce a turbulent boundary layer artificially by roughening the nose tip of the model unless the entry pitch angle is nose up enough to cause the ogive to contact the water first.

3. If the entry velocity of the model is high enough to cause a turbulent boundary layer, the behavior of the model is unaltered by the roughness on the nose tip.

4. Because of the difficulties associated with causing a turbulent boundary layer by artificial means, it is preferable to conduct modeling experiments at entry velocities which will cause the turbulent boundary layer to occur naturally.

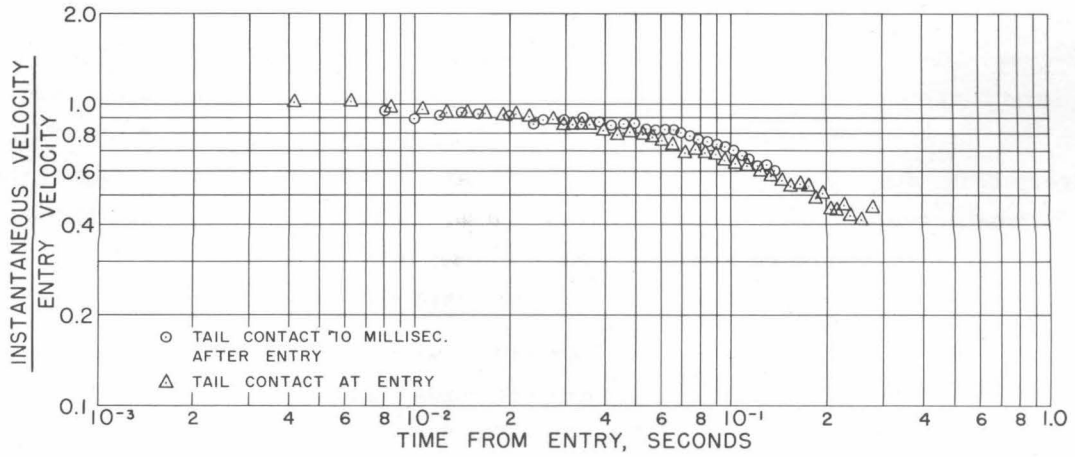

Fig. 27 - The ratio of instantaneous velocity to entry velocity as a function of time. Entry velocity of smooth model: 60 fps. Air pressure: 1/11 atm.

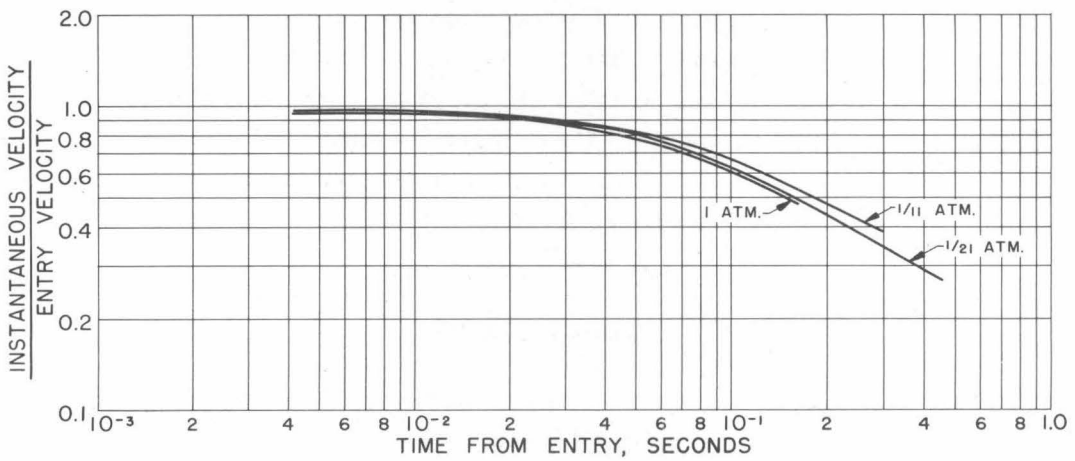

Fig. 28 - The ratio of instantaneous velocity to entry velocity as a function of time. Entry velocity of model: 60 fps.

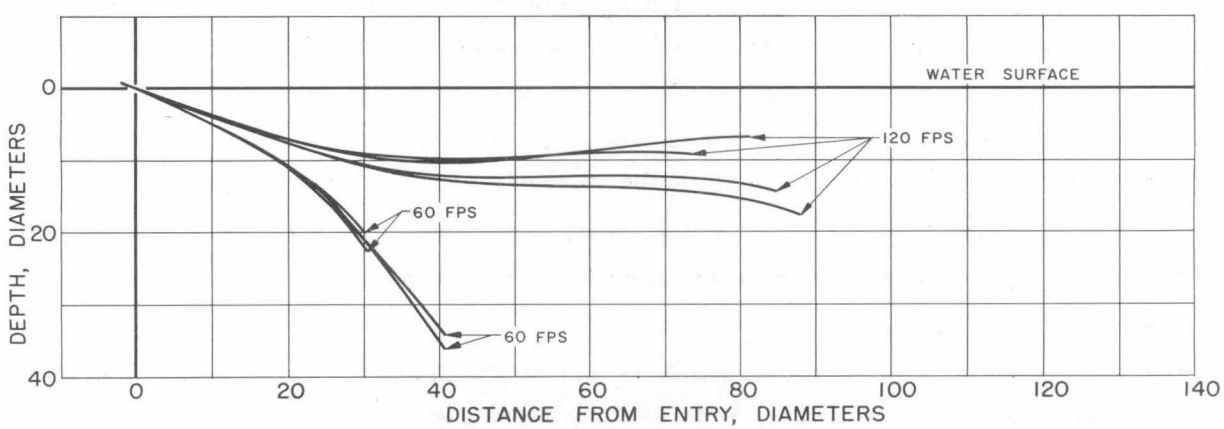

Fig. 29 - Underwater trajectories of smooth model - Entry velocities: 60 and 120 fps. Entry pitch angles: 0.6° nose down to 0.4° nose up. Air pressure: 1/11 atm.

5. Surface tension forces are insignificant in this equal cavitation number-Froude scaled system. (See Item 2 below.)

6. Care should be exercised in extrapolating from the behavior of a particular shape under rather limited entry conditions.

B. Behavior of the Model Alone

1. Contact of the tail with the bottom of the cavity does not necessarily cause an upturning trajectory.

2. At full atmospheric pressure the forces of surface tension did affect the behavior of the roughened model.

3. The deceleration of the model was not significantly altered by:

   (a) Change in air pressure.

   (b) Change in entry pitch angle.

   (c) Change in the time of initial contact between the tail and the cavity wall.

4. The deceleration of the model was a function of entry velocity.

APPENDIX

A. PROTOTYPE LAUNCHINGS:

Angles Measured to $\pm 1^{o}$

Velocity Measured to ± 5 fps

Run No. (Val.)	Air Trajectory Angle Degrees	Entry Pitch Angle Degrees	Entry Velocity fps
620	20.2	0.7 nose down	414
711	23.0	1.1 nose up	200(nom.)
712	22.8	1.0 nose up	193
715	22.5	0.3 nose down	197
717	20.0	0.1 nose down	200(nom.)
718	20.0	0.1 nose up	195
720	22.5	0.8 nose up	201
722	22.2	0.4 nose up	202
727	22.2	2.1 nose up	200
728	22.2	1.7 nose up	202
750	22.1	2.2 nose up	207
751	22.2	1.6 nose up	209
769	21.6	1.9 nose up	213
771	21.5	0.3 nose up	206
780	22.6	2.8 nose up	204
781	22.7	2.7 nose up	198
1558	23.7	2.5 nose up	183
1559	23.7	2.4 nose up	198
1612	23.5	5.8 nose up	189
1615	23.3	3.0 nose up	187
1619	23.2	2.7 nose up	214
1627	20.0	5.9 nose up	194

APPENDIX

B. MODEL LAUNCHINGS - VAVP TANK, NOTS, FOOTHILL

Entry Angles (nominal): 20° Air Trajectory
0.5° Nose Down Entry Pitch

Entry Angles (actual): $\pm 0.5^{\circ}$ of Nominal Angles

Run No.	Entry Velocity fps ±1/2 fps	Air Pressure Atm.	Roughness Type	Surface Tension Dynes/cm
769	80.8	1/11	B	76
770	81.2	1/11	-	76
771	81.4	1	-	76
772	61.4	1	-	76
773	61.2	1/11	-	76
774	61.4	1/11	B	76
775	61.8	1	B	76
776	80.8	1	B	76
777	60 (nom.)	1/11	-	76
778	61.2	1/11	-	76
779	61.7	1	-	76
780	61.4	1	B	76
781	61.7	1	B	76
782	61.4	1	B	76
783	81.0	1	B	76
784	81.2	1	B	76
785	81.7	1	B	76
786	81.0	1/11	-	76
787	80.7	1	-	76
788	81.0	1/11	B	76
789	81.3	1/11	B	76
790	61.2	1/11	B	76
791	61.4	1/11	B	76
792	61.5	1	B	39.8
793	60 (nom.)	1	B	39.8
794	62.4	1	B	41.8
795	62.1	1	B	39.2
796	61.7	1/11	B	40.1

APPENDIX

C. MODEL LAUNCHINGS - CALT, HYDRODYNAMICS LABORATORY

Run No.	Air Trajectory Angle Degrees	Entry Pitch Angle Degrees	Tolerance on Angles Degrees	Entry Velocity fps ±1/2 fps	Entry Pitch Velocity Deg/Sec	Air Pressure Atm.	Roughness Type
74	23.3	2.2 nose up	1	59.3		1	-
75	22.4	1.3 nose up	1	61.3	5 nose down	1/11	-
76	22.7	0.2 nose up	1	60.3	5-10 nose down	1/11	-
77	22.4	0.2 nose up	1	60.4	10 nose up	1/11	-
78	23.1	0.4 nose up	1	59.6	20 nose up	1/11	-
79	22.3	2.4 nose down	1	60.0	10 nose down	1/11	-
80	22.6	1.0 nose down	1	60.5	10 nose down	1/11	-
81	22.4	0.2 nose up	1	61.0	15 nose up	1/11	-
82	22.2	1.4 nose up	1	60.6	10 nose up	1/11	-
83	22.5	2.5 nose up	1	60.6	25 nose up	1/11	-
84	22.3	2.1 nose up	1	60.2	0	1/11	-
85	21.4	3.5 nose up	1	61.1	10 nose up	1/11	-
86	21.3	4.2 nose up	1	60.6	10 nose down	1/11	-
87	21.2	4.2 nose up	1/2	60.1	5 nose down	1/11	-
88	21.3	5.0 nose up	1/4	60.1	0	1/11	-
89	20.8	1.0 nose up	1/2	60.6	0	1/21	-
90	20.8	1.1 nose up	1/2	60.9	10 nose up	1/21	-
91	21.3	5.4 nose up	1/4	60.3	5 nose down	1	-
92	20.6	4.4 nose up	1/4	60.6	10-15 nose down	1	-
93	20.6	2.6 nose up	1/4	60.0	0	1	-
94	20.6	0.8 nose up	1/2	60.6	0	1	-
95	21.1	2.1 nose up	1	60 (nom.)	-	1/11	A
96	20.9	1.9 nose up	1/2	60.1	0	1/11	A
97	21.0	1.2 nose up	1/4	60.8	5 nose up	1/11	B
98	22 (nom.)	1-1/2 nose up (approx.)	-	60 (nom.)	-	1/11	B
99	20.8	1.6 nose up	1/2	59.9	10 nose up	1/11	B
101	20.0	0.0	1/4	120.2	10 nose down	1/11	-
102	19.9	0.3 nose down	1/4	120.0	10-15 nose down	1/11	-
103	17.7	2.9 nose down	1/4	122.4	25 nose down	1/11	-
106	21.0	1.5 nose up	1/2	60.0	10 nose down	1/11	B
107	21.0	1.6 nose up	1/2	60.4	10 nose down	1/11	B
108	21.2	5.4 nose up	1/2	60.2	10 nose down	1/11	B
109	21.2	0.5 nose down	1/2	120.5	-	1/11	B
110	21.1	1.0 nose down	1	120.0	30 nose down	1/11	B
113	21.6	6.2 nose up	1/4	60.9	5 nose down	1/11	B
114	21.3	0.2 nose down	1/2	119.8	10 nose down	1/11	B
115	21.5	0.4 nose down	1/4	121.0	5 nose down	1/11	-
116	21.5	0.6 nose down	1/2	120.6	10 nose down	1/11	-
117	21.6	1.9 nose up	1/4	60.2	5 nose up	1/11	C
119	21.5	5.4 nose up	1/2	60.3	15 nose down	1/11	D
120	21.1	5.2 nose up	1/2	60.1	10 nose down	1	D
121	21.3	5.2 nose up	1/4	60.2	25 nose down	1/11	E
122	19.0	1.0 nose down	1	60.8	15 nose down	1	B
123	19.9	0.1 nose up	1	60.2	20 nose down	1	B
124	19.0	0.9 nose down	1	60.2	15 nose down	1	B
126	19.1	1.0 nose down	1	60.8	15 nose down	1	B
129	20.1	0.2 nose down	1/2	120.5	15 nose down	1	B
130	20.2	0.1 nose down	1/2	121.0	20 nose down	1	B
131	20.0	0.1 nose down	1/2	120.9	-	1	B

BIBLIOGRAPHY

1. Levy, Joseph and Kaye, John, "Effect of Atmospheric Pressure on Entry Behavior of Models of the Mark 13-6 Torpedo with Standard Head (Head F) and One Finer Head (Head I)," California Institute of Technology, Hydrodynamics Laboratory Report No. N-59, January 1949.

2. Levy, Joseph and Kaye, John, "Preliminary Studies of Effect of Atmospheric Pressure on Trajectory of 2-Inch Correlation Model of Mark 13-6 Torpedo," California Institute of Technology, Hydrodynamics Laboratory Report No. M-59, March 1948.

3. Knapp, R. T., "Nose Cavitation on Ogives and Spherogives," OSRD Section No. 6.1-sr207-1906, Hydraulic Machinery Laboratory Report No. ND 31.1, January 1945.

4. Jennison, James H., "The Variable-Angle Launcher for Air-To-Water Missiles," Navy Dept., Bureau of Ordnance, Naval Ordnance Test Station, Inyokern Report No. 1180, May 15, 1950.

5. Smith, J. A., "Variable Angle Launcher," Navy Dept., Bureau of Ordnance, Naval Ordnance Test Station, Inyokern, Report No. 1327, June 16, 1952.

6. "Activities of the Underwater Ordnance Department," Navy Dept., Bureau of Ordnance, Naval Ordnance Test Station, Inyokern, June 1951.

7. Knapp, R. T., Levy, J., O'Neill, J. P., and Brown, F. B., "The Hydrodynamics Laboratory of the California Institute of Technology," Trans. Am. Soc. Mech. Engrs., Vol 70, No. 5, pp. 437-457, July, 1948.

8. Waugh, J. G., "Water Entry Whip and Deceleration of Eight Full-Scale Torpedo Models with Ogive and Spherogive Heads," Navy Dept., Bureau of Ordnance, Naval Ordnance Test Station, Inyokern, Report No. 1223, March 2, 1950.

9. Wilcox, G. M., "Drag Studies in Water Entry of the Mk 13-6 Torpedo," California Institute of Technology, Hydrodynamics Laboratory Report No. E-12.1, July 1951.